As a result of the review process, the manuscript has been modified significantly. Mayor changes are:

1) Section 2 of the paper has been extended to include a brief but detailed description of the TropOMAER algorithm. It includes a description of the UVAI calculation as well as a summary of the AOD/SSA retrieval process.
2) Section 3 on the validation of retrieval results using AERONET observations also changed considerably. The original validation analysis consisting of a direct validation of TROPOMI AOD results to AERONET observations at 12 sites was replaced with an approach that allows the separate evaluation of retrieved product improvement as a result of instrument enhancement and algorithmic improvement. AERONET observations 12 sites are used as an aggregate. A three way validation exercise is then carried out: 1) AERONET vs OMI, 2) AERONET vs TROPOMI using heritage (OMI) cloud mask, and 3) AERONET vs TROPOMI using VIIRS-based cloud mask. Inter-comparison for validations 1 and 2 highlights the effect of improved instrumental capabilities, whereas differences in validations 2 and 3 indicate retrieved product improvement due to algorithmic upgrades.
3) The revised paper (to be available soon after the submission of replies to reviewers' comments) contains 13 figures (five more than in the original version).

In the reply below the reviewer's comment is in black and our answer in blue.

Reply to Comments by Reviewer 1

Summary:

This manuscript introduces the TropOMAER aerosol retrieval algorithm. The algorithm is essentially the heritage OMAERUV algorithm from the OMI collection, now modified to be applied to TropOMI data instead. In this adaptation process, the ability to retrieve above cloud aerosol OMACA has been included. The introduction to the algorithm itself is quick. The authors point out two major differences from OMAERUV: (1) TropOMI's finer spatial resolution (2) still evolving radiometric calibration. There is a quick evaluation section showing TropOMAER retrievals against 12 selected individual AERONET stations for aerosol optical depth (AOD) and an aggregation of all 12 stations for single scattering albedo (SSA). Then the bulk of the manuscript demonstrates TropOMAER in three interesting and newsworthy biomass burning events.

We thank the reviewer for his/her comments that have contributed to an improved manuscript.

Assessment:

There is much merit in this manuscript. The three examples, especially the third example, are scientifically extremely interesting. However as currently written, it is missing too much detail for publication in AMT. AMT is where algorithm developers, such as these authors and myself "talk shop", and where we document the details of algorithms and validity of our products. While the heritage algorithms are well-documented in the literature, porting an algorithm to a new sensor introduces new challenges that are very interesting to other algorithm developers and should be included in a paper like this one. This manuscript could easily be adapted into a form that would be appropriate for AMT, if that is what the authors want to do. These are the points that would make the manuscript ready for publication in AMT:

(1) much more description of the algorithm itself, even if that description were partly reiterated from previous publications.

The section on algorithm description was extended to elaborate on key aspects of the inversion scheme.

(2) highlight differences between OMI and TropOMI instruments, between OMIAERUV and TropOMAER algorithms, most importantly between results from each sensor.

The purpose of the comparison to AERONET has changed from the narrowly focused AOD validation exercise in the original version of the paper, to an analysis of the instrumental and algorithmic differences throughout the use of independent ground-based observations. The combined AERONET data aggregate from observations the 12 sites, is compared to satellite observations as follows. An evaluation of instrument-related and algorithmic improvements is done by comparing AERONET measurements to three satellite-based data sets:1) OMAERUV, 2) TropOMAER with heritage (i.e., OMAERUV) cloud screening, and 3) TropOMAER with VIIRS cloud mask.
A comparative analysis of evaluations 1 and 2 shows the impact of enhanced instrumental capabilities, whereas the analysis of evaluations 2 and 3 highlights the effect of using the VIIRS cloud mask which is the only TropOMAER algorithmic modification.

Of prime interest to potential users of TropOMAER products who have been using OMI products is how do the products from the new sensor compare with the products from the old sensor. The only place I see a hint of that is the plotting of OMI retrievals with TropOMI

retrievals on the time series in Fig. 5. However, that figure is not satisfying. Much more interesting than the 15-year time series would be a difference time series during the TropOMI era and a scatter plot of TropOMI against OMI, even on a monthly mean basis.

The parallel validation of OMI and TROPOMI described above addresses this issue.

As suggested, the consistency of the OMAERUV and TropOMAER records are evaluated by comparisons between the products at different time scales:

OMI-TROPOMI visual inspection comparisons of UVAI are shown on Figure 1 for the smoke plume over North America on August 18, 2018. This comparison also includes the KNMI TROPOMI UVAI.

Side-by-side maps of OMI and TROPOMI retrieved SSA and AOD for the same event are also shown on Figure 8.

A two-year time series of monthly-averaged OMI and TROPOMI AOD and AAOD over three regions are shown on Figure 4.

OMI and TROPOMI summer seasonal global maps are compared in Fig 6, and a scatter plot of OMI-TROPOMI monthly UVAI values is shown on Figure 7.

(3) evaluation of TropOMAER should be expanded. There should be an effort to trace the consequences of the finer spatial resolution and issues with calibration to the evaluation. Right now the authors skirt these issues without really proving anything. For example they mention subpixel cloud contamination being absent in most validation sites. However, when I look at the 12 panels in Figure 1, I see no qualitative difference between the 3 sites mentioned as having subpixel cloud contamination and the other 9 sites. If there was marked improvement from Ahn et al., 2014, then that improvement should be demonstrated in this paper. I should not have to call up that paper and run my eyes between two different figures in two different papers to see the improvement.

The effect of the only implemented algorithm improvement (VIIRS cloud mask) has been addressed in our reply to comment (2) above.

Later they mention needing a finer resolution surface albedo map, and there is also mention of the calibration causing some of the offset in the validation plots. Each of these issues is very interesting to another algorithm developer, like myself, or to potential users of the products. AMT is the right journal to present an analysis of these issues, and prove their consequence on the retrievals. Currently that analysis is missing.
In principle, as discussed in the manuscript, the identified AERONET-TropOMAER positive AOD bias (~0.2) could be the result of remaining calibration offset and/or issues with the coarse resolution of the currently used surface albedo data base. A calibration error will affect all AOD retrievals (independently of AOD magnitude) whereas a surface-albedo related error will impact retrieved low AOD values (up to ~ 0.5). At larger AOD's surface-albedo-related effect become increasingly smaller. Specific conclusions regarding the magnitudes of these effects in TropOMAER are not yet available as we continue to investigate them. The discussion following the validation analysis includes these considerations.

(4) Slow down and present the details. I felt that there was a rush through the "boring" algorithm piece of the paper in order to get to the "exciting" demonstration with the big biomass burning events. There are many details left behind in the rush: There are many acronyms never properly introduced:

p.2 line 2 should put (SWIR) after shortwave infrared.

Done

P2 line 5. ESA and DLR?

Done

P2 line 28. Should put (ALH) after aerosol layer height

Done

P5 line 5. UVAI is never defined as an acronym, and worse, it is never defined as a product. Suddenly it is being shown in figures and being used as a fundamental part of the analysis.

This shortcoming has been addressed in the added algorithm description section.

P6 line 25 SAM?

Stratospheric Aerosol Mass

P6 line 33. What are total mappers?

Nadir looking full daily coverage sensors (no longer in the discussion)

The concepts of Level 1 and Level 2 data are not explained (p2 line 5).

Done

Exactly what AERONET data are we looking at? Version 2 or 3? Levels 1.5 or 2? There is no explanation that AERONET AOD has a documented uncertainty of 0.02 in the UV, but that the SSA retrieval is a retrieval with much broader error bars. There is no explanation of why or how these 12 stations are selected, nor what the time range we are looking at.

Version 3 Level 2 data

(5) Provide more detail in the demonstration section. Figure 3 would benefit greatly by adding a swath just to the west of the swath shown. Right now there is a lot of description of fires and smoke in California, the Pacific Northwest and British Columbia, but none of those areas are shown in the figure. Only the areas downwind.

Added another orbit as suggested.

P6. Lines 1 to 6. Is this method here the manifestation of the ACA part of the TropOMI retrieval that is mentioned at the beginning? If so, then please make that clear. If it is a different method, then explain

why the referenced ACA method is not used. If not, then is there any demonstration of the ACA TropOMI method? ACA is an important new addition to OMIAERUV, and should be highlighted or discussed if this is going to AMT.

It is the same. Stated in the manuscript.

P6 Line 10. The extinction-to-mass conversion is important. The appendix should be referenced here.

Done

P6 lines 13-16. Is there a physical basis for this? This is important, and how the UVAI AOD relationship relates to height, and especially to height in the stratosphere needs to be explained. Remember that UVAI jumps in suddenly with no introduction. It would be worthwhile to take the time to explain it, and some of the physics behind the whole interrelationship between height, AOD, UVAI and absorption. Maybe in Section 2?

For given values of ALH and AAE, UVAI increases rapidly with aerosol load up to AOD values in about the range 4-6 when it starts to saturate. At these large AOD's the aerosol absorption of Rayleigh scattered light peaks, and further UVAI enhancements are only possible for increased values of ALH and/or aerosol absorption exponent (AAE). Thus, for AOD values larger than about 6, and known or assumed AAE, the UVAI effectively becomes a measure of ALH. As suggested, this discussion has been included in section 2, where the UVAI concept is first introduced.

P6 line 25 to P7 line 2. A lot of numbers are given here and these are means with uncertainties surrounding them. The uncertainty is given at the end of±40%. It would be helpful to explain how the mean is derived (for what density) and what is the interplay between assumptions of density and uncertainty in height.

We meant uncertainty in AAE. ALH is given by CALIOP.
The uncertainty of the estimated stratospheric aerosol mass (SAM) is ±40% which represents the combined effect of uncertainties on assumed AAE (4.8±0.5) in the AOD retrieval, and the uncertainty in assumed aerosol density in the range 0.79 and 1.53 g-cm−3, which covers the range of values reported in the literature (Reid et al., 2005). For simplicity, we assume a midrange aerosol mass density value of 1.16 g-cm−3. These details are part of the discussion in the revised manuscript.

P7 lines 27-33. This is very interesting, but the figure doesn't really portray this information well. Figure 5 needs to become more informative.

(6) All the captions need to more descriptive. Be sure to give details on specific data, be sure to describe what is shown in each panel, what wavelength is being shown, what temporal resolution is being plotted (fig. 5), what do each of the colors in the color bars represent. But in general a LOT more information needs to be in the figure captions.

We assume the reviewer means fig 8.
Figure 13 (previously Fig 8) shows calculated daily values of aerosol mass (in kilotons) from December 31, 2019 thru January 7, 2020, resulting from aerosols above 12 km, altitude used as a proxy of the tropopause height. Separate aerosol mass retrievals were carried out for cloud free (blue bars) and cloudy scenes (green bars), with the daily total stratospheric aerosol mass given as the sum of these two components (orange bars).

Suggestion: It occurred to me that this manuscript might fit a “letters” journal much better. Right now it is not too long. The authors would need to triage their figures down to 4. Perhaps Figs. 1, 3, 5 (with a bottom panel showing the difference between TropOMI and OMI) and 8. Then the very short description of the algorithm, evaluation and methods would be appropriate, and the purpose of the paper is NOT to describe TropOMAER, but to illustrate these biomass burning events. The point of the paper shifts from an “atmospheric measurement technique” to a better understanding of the Earth’s atmospheric phenomena. GRL would be a possibility, but also ERL.

Thanks for the suggestion. We decided to stay with AMT

Reply to Comments by Reviewer 2

This paper briefly introduces a TropOMI aerosol data set based on heritage OMI UV algorithms by the Torres group (OMAERUV and OMACA). This provides UV aerosol index (UVAI), aerosol optical depth (AOD), and single scattering albedo (SSA). A comparison of AOD and SSA against data from selected AERONET sites is presented, along with a few case studies of extreme events. The concept of the paper is in scope for AMT. The quality of language is good. The topic is important because OMI is ageing and TropOMI is the next generation of this type of sensor (OMPS on SNPP and JPSS has some aerosol capabilities but is in other ways worse than OMI).

However, honestly, the current paper feels more like a conference proceedings or an article for a Letters journal than a full scientific paper. It is brief and does not go into much detail. For a focused journal like AMT I think something much more technical is needed. Though I realise I am proposing a fair amount of work, I prefer that the authors expand this analysis rather than resubmit elsewhere, because I think a thorough accounting for TropOMI's capabilities for UV aerosol remote sensing is needed and is Interactive more or less missing from the literature. The authors are the right people to do this comment because they are the most expert with their data products. I know it is annoying when reviewers ask to do more work, but there is not enough content here to justify publication and I don't think that the article as written satisfies the scope a reader would reasonably expect. Case studies are one thing but by nature are typically unusual events and so looking at them may not give a representative picture of the data set as a whole. I recommend major revisions and would like to review the revision.

The paper has been significantly extended to address the issues raised in the review process.

My main suggestion for expansion is to give a detailed comparison between OMI and TropOMI results.

The original evaluation analysis involving AERONET-TROPOMI comparison of aerosol derived products have been converted into a three-way AERONET-TROPOMI-OMI over the same period.

OMI-TROPOMI results are compared for individual events as well as in terms of monthly averages for three representative regions as well as seasonal (summer) global averages.

Users familiar with OMI need to know whether we can use TropOMI for the same types of research, and to what extent the same caveats/biases are found. Right now this is not answered in a thorough way. One big advantage of TropOMI over OMI is the spatial resolution. I would expect that this is important because those cases where the UV technique works well (absorbing aerosols) are also often strong and heterogeneous events. So the finer spatial resolution might mean both (1) less cloud contamination and (2) better AOD/SSA retrievals, because top of atmosphere radiance is not linear in AOD, so by resolving more spatial structure you become less sensitive to sub-pixel variations. If this is true in practice, great. If not, this needs to be shown and understood. It is briefly discussed in Section 3.1 but not supported by the plots shown, only by briefly mentioning other references. Here are some suggestions for relevant analyses to include:

The revised version of the paper specifically addresses the issues addressed by the reviewer as explained below.

(1) Show global maps so we can see how similar the big picture looks from both sensors. In my view the time series in Figure 5 isn't sufficient here because both data sets are heavily spatially and temporally averaged in it.

Because of the so-called row anomaly of the OMI sensor that reduces OMI's daily coverage to about 50%, OMI-TROPOMI global daily maps are not the best way visual comparison. We show OMI-TROPOMI comparison on daily, monthly regional, and global seasonal temporal scales.

In Figure 1 of the revised version of the manuscript we show a comparison of OMI, NASA-TROPOMI and KNMI-TROPOMI UVAI on August 18 over North America. To our knowledge, except for UVAI, no other TROPOMI aerosol products are available.

Side-by-side maps of OMI and TROPOMI retrieved SSA and AOD for the same event are shown on Figure 8.

A two-year time series of monthly-averaged OMI and TROPOMI AOD and AAOD (absorbing aerosol optical depth) over three regions are shown on Figure 4.

OMI and TROPOMI summer 2018 seasonal global maps are compared in Fig 6, and a scatter plots of OMI TROPOMI UVAI monthly mean values is shown on Figure 7.

(2) Include OMI in some of the case studies (e.g. visual inspection of maps).

OMI graphics similar to the TROPOMI images have been added to the discussion of the 2018 California and Pacific northwest fires.

(3) OMI validation results could be presented alongside the TropOMI data. I know the validation has been published elsewhere but it will be clearer to the reader if plots are shown next to one another with the same axis range, etc.

The focus of the comparison to AERONET has changed from the narrowly focused AOD validation exercise in the original version of the paper, to an analysis of the instrumental and algorithmic differences throughout the use of independent ground-based observations. The combined AERONET data aggregate from observations the 12 sites, is compared to satellite observations as follows. An evaluation of instrument-related improvements is done by comparing AERONET measurements to three satellite-based data sets:1) OMAERUV, 2) TropOMAER with heritage (i.e., OMAERUV) cloud screening, and 3) TropOMAER with VIIRS cloud mask.

A comparative analysis of evaluations 1 and 2 shows the impact of enhanced instrumental capabilities, whereas the analysis of evaluations 2 and 3 highlights the effect of using the VIIRS cloud mask which is the only TropOMAER algorithmic modification.

(4) Directly plot (as a scatter density diagram) the AOD and/or UVAI from OMI and TropOMI, for collocated pixels (i.e. same scene, same time, similar geometry) at level 2 resolution. The orbits should overlap frequently. Then we can see if there's much scatter, if it's a straight line or not, etc. I don't know how much collocated data is needed to get a meaningful comparison – perhaps the case studies give enough, perhaps it has to be done on a month's worth of data. MODIS or VIIRS data could be useful for extra context (and filtering); I know and the manuscript mentions that the TropOMI orbit choice makes it possible to take advantage of SNPP VIIRS for e.g. cloud masking.

Because of the row anomaly the orbital overlap the reviewer describes is very cumbersome and time consuming. Figure 7 shows a scatter plot of seasonally averaged UVAI for the data mapped in Figure 6.

We believe the OMI-TROPOMI comparative analysis at daily, monthly regional, and seasonal temporal presented offers a complete analysis of the equivalence and compatibility of these two data sets. Additional comparisons involving other sensors are beyond the scope of this manuscript intended as a paper on first results of the ported algorithm and not yet a consolidated product.

The above comments and suggestions all apply (potentially) to the DSCOVR-EPIC sensor, too, although OMI is the more well-known and mature record so probably makes better sense to baseline against. Though I would certainly be happy to see a three-way (OMI, EPIC, TropOMI) comparison.

We will certainly carry additional comparison to other satellite products in the near future.

Other comments on the study are as follows:

Introduction or section 2.1: somewhere here it would be good to contrast TropOMI capabilities (e.g. spatial/spatial) with OMI and maybe TOMS and EPIC, since those are the main comparative products. The introduction mentions GOME and SCIAMACHY but those are less relevant since the authors' algorithms are from TOMS/OMI heritage and EPIC data are shown later. Maybe mention OMPS too as while a step backwards from OMI in terms of spatial resolution, it is used for UVAI and is the US operational follow-on for that. I know that there are TropOMI products in development on the Dutch side too – it's not clear to me whether those are public yet, but if so, there may be value in comparing and contrasting with those too.

The TOMS, EPIC and OMPS records are included in the discussion.

Section 2.2: if I understand correctly this section states that (1) there is a 5-10% calibration difference between OMI/OMPS and TropOMI in the relevant bands in the standard calibration, and (2) because of this the authors do their own vicarious calibration. Is that right? Either way, this could be worded a little more clearly. What is the difference between the sensors after the vicarious calibration?

The vicarious calibration brings the TROPOMI and OMI closer in measured reflectance terms as evidenced by the AOD validation presented here that shows overall consistency between the two records. The revised version of the manuscript contains an improved description of the vicarious calibration procedure.

Section 3: clear statements and references about AERONET data products and versions used need to be made. For example, I assume this is version 3 level 2.0 direct Sun (Giles et al AMT 2019) and inversions (Sinyuk et al AMT 2020). However this does not appear to be actually stated in the paper. If this was not the versions used, the analyses should be repeated using the latest data versions.

Yes, AERONET data version 3, level 2.0 was used. It has been clearly stated in the revised version of the paper.

Section 3.1: if the authors really believe that a relative uncertainty of 30% on TropOMI AOD is true, then by definition they should not be using linear least squares regression fits, because a relative uncertainty means that the assumption of constant variance of errors is broken. See for example standard statistics textbooks or web pages such as https://statisticsbyjim.com/regression/heteroscedasticity-regression/ . This issue could be addressed with weighted least squares. Ideally also the uncertainty on AERONET AOD (I think 0.02 in this spectral region) should be accounted for in the fitting. Also, if you expect a relative uncertainty then RMSE is not the best metric to be reporting since that is scale-dependent…others like relative RMSE would be more appropriate to quote instead/as well (and this would help tell you if it is really 30%). The statistical analysis here is not very appropriate. The authors may have used this type of analysis before but that does not mean it is ok to do something again if it is wrong.

TROPOMI's retrieval uncertainty is probably lower than the quoted 30% value. This is actually a conservative TOMS/OMI based estimate that includes the combined effect of the uncertainty on assumed aerosol layer height (smoke and dust layers) and sub-pixel cloud contamination. At TROPOMI's much finer spatial resolution the cloud contamination component should be significantly lower. Actual uncertainty is still to be determined pending remaining calibration issues as discussed in this manuscript. We appreciate the reviewer's observation on the appropriateness of using linear square regression (LQR) fits . LQR analysis have been used as a standard method of validating satellite AOD retrievals The use of this common approach facilitates the relative comparison of the same physical parameter measured by large variety of sensors and retrieval algorithms.

The reported LQR parameters in this manuscript based on relatively small sample of observations are only intended to illustrate relative improvement in the accuracy of retrieved parameters associated with TROPOMI enhanced instrumental and algorithmic capabilities with respect to OMI. We do not expect the conclusion of our analysis to change if a more refined fitting approach was used. This is by no means an exhaustive validation exercise of the TROPOMI record for which a lot more AERONET observations are needed.

Section 3.2: the authors use a 6 hour time window (3 hours each side) for the SSA comparison because morning/evening almucantar inversions have lower uncertainty than midday ones. The untested assumption here is that SSA does not vary much throughout the day. Ok, but version 3 also introduced hybrid scans which were specifically developed to solve this problem by sampling a larger air mass and scattering angle range during the middle of the day. This could be checked by using the hybrid inversions as well and seeing if you get the same results.

Hybrid scan availability is limited to specific sensor types. In general, reliable AERONET SSA retrievals are done for AOD (440 nm) > 0.40. That limitation significantly reduces the number of SSA measurements available for comparisons to satellite retrievals. Using hybrid scans only further reduces data available.

The hybrid scans are certainly useful to examine the issue of diurnal variability. We will consider using them in future specific validation efforts.

Also, an explanation is needed for how the authors split the data into the three aerosol type categories for Figure 2 and the discussion.

The aerosol typing is described in a new section of the paper that describes the algorithm as suggested by reviewer 1

Section 4: this feels like advertising. I agree that TropOMI results look impressive but (aside from a brief mention of AERONET AOD) there is no way to know how 'real' they are. This section feels like something you might put on a webpage or brochure to attract attention to your new data set, rather than a detailed scientific analysis. I am not sure what is best to do here. For a journal like AMT I'd rather than space was devoted to more technical, large-scale comparisons. Perhaps this aspect could be split off for a Letters journal. Or, expanded with more context from meteorology and other (space or suborbital) data records and submitted separately to ACP. I know this is a joint special issue but the content still needs to match the journal. It does not really fit here, and there's not enough detail presented to consider this paper an authoritative reference for these case studies.

We disagree with the negative connotation of the term 'advertising' as used by the reviewer. As a matter of fact, this entire paper, not just section 4, as well as all science papers, are intended to introduce and advertise the availability of a new science products or ideas. That is the role of the scientific literature. The problem is when false advertisement takes place. Hopefully, the preceding three sections of the paper on algorithm description and evaluation of derived products give the reader some confidence to treat as 'real' the discussed practical applications of the derived products in section 4.

Figure 6 and associated text: I'm not sure that it makes sense to show the EPIC results on the left panel. That's a different sensor, different resolution, different observation geometry (backscatter for EPIC). UVAI is sensitive to all of these things. Also, what is the scaling referred to in the left panel? That is not mentioned in the paper.

Left panel Figure 6 has been excluded as it does not add much to the discussion without going into an additional explanation and description of the EPIC sensor. The EPIC application referred to in this paper is discussed in detail in the quoted literature.

I expect that the general point about the two events will still stand but it's not clear how much of the systematic difference (and scatter on the left panel) are a function of real differences in the smoke in the two events and how much is contributed by sensor differences. The paper is far too sparse in detail for a reader to judge, which makes the comparison less instructive.

Figure 6 left panel has been removed.

Figure 6 legend: is the black dot in the left panel legend (12 km) meant to be a black line like in the right panel? If so, formatting should be consistent. If not, the difference needs to be explained.

Figure 6 left panel has been removed.

Section 5: "The NASA TropOMAER aerosol algorithm is a modified version of the one applied to OMI observations." Wait, what? Section 2 describes the OMI approach but doesn't clearly state that there are modifications. What are these modifications, why were they made, what effect does this have on the results, and will they be back-ported to OMI? This all needs to be addressed in the paper.

Do not panic. The only modification is the use of the VIIRS cloud mask whose effect in retrieval results has been discussed.

Reply to Comments by Reviewer 3

This paper presents NASA aerosol product for TROPOMI obtained with TropOMAER retrieval algorithm. In general, the manuscript is well-written, well-structured and demonstrates the possibilities of TropOMAER retrieval algorithm. First, the AOD and SSA products were evaluated using AERONET dataset for 12 representative sites. Then, the results of the algorithm application to a few important aerosol events were presented and total aerosol mass injection was estimated. There are few remarks regarding AOD and SSA validation against AERONET.

1. Figure 1 and Table 1 clearly indicate the presence of positive bias in TropOMAER AOD product at 380nm over all 12 representative sites. Authors already provided some guess about the origin of this bias and mention that this issue is under investigations. Nevertheless, since the retrieval is carried out at 388 nm, and reported also at 354 and 500 nm, presenting AOD validation results in the manuscript for two wavelengths (for example, 380 and 500 nm) would be very useful to address the bias issue.

The TropOMAER reported 354 and 500 nm AOD values are obtained by direct conversion from the retrieved 388 nm product that is based on the assumed spectral dependence of the aerosol models. We do not think the small wavelength difference between the AERONET 380 nm, and the satellite reported value at 388 nm explain the reported difference in the comparison. In regard to the evaluation at 500 nm, the added uncertainty of the reported AOD associated with the wavelength dependence would only make the interpretation of results more complicated. The suggestion, however, is very good and will be considered in upcoming evaluations of TropOMAER results.

2. One of the parameters of AOD evaluation is 30% matchup criteria. What is the origin of these criteria? Is AOD product with 30% uncertainty sufficient for trace gases retrieval? For example, GCOS requirements on AOD are much more strict: 0.03 or 10%.

TROPOMI's retrieval uncertainty is probably lower than the quoted 30% value. It is not, however, used as a matchup criterion. This value is actually a conservative TOMS/OMI-based estimate that includes the combined effect of the uncertainty on assumed aerosol layer height (smoke and dust layers) and sub-pixel cloud contamination. At TROPOMI's much finer spatial resolution the cloud contamination component should be significantly lower. Actual uncertainty is still to be determined pending remaining calibration issues as discussed in this manuscript.

3. The results of SSA validation show reasonable correspondence with AERONET. Nevertheless, Figure 2 clearly shows overestimation of SSA especially for absorbing aerosol when SSA from AERONET < 0.9. Is this related to the same issues providing positive bias in AOD? Is this SSA overestimation a demonstration of limitation of aerosol model used in TropOMAER algorithm? More discussions here are necessary.

The revised version of the paper includes parallel AERONET-OMI and AERONET-TROPOMI evaluations of both AOD and SSA products. The observed apparent overestimation of the satellite SSA values for desert dust aerosols is also present in the OMI comparisons (Figure 3a) and has been discussed in published literature (Jethva et al., 2014). Such overestimation, however, is not as clear in the presence of carbonaceous aerosols. The larger-than-AERONET desert dust SSA values (when AERONET < 0.9)

are also observed in the TropOMAER evaluation for both the heritage (Figure 3b) and VIIRS (Figure 3c) cloud screening approaches. A smaller but observable similar effect is also apparent in the TROPOMI evaluation, suggesting a possible connection with lingering sensor calibration issues.

In general, I would recommend authors to reserve some space in the manuscript for discussions regarding identified issues in the retrieval. For example, the mentioned above issues for AOD and SSA retrieval as well as authors thoughts how to treat these issues would be highly appreciated by broad remote sensing community. These discussions would greatly increase the scientific strength of the paper.

These issues are discussed in the revised version of the manuscript.

TROPOMI Aerosol Products: Evaluation and Observations of Synoptic Scale Carbonaceous Aerosol Plumes during 2018-2020

Omar Torres[1], Hiren Jethva[2], Changwoo Ahn[3], Glen Jaross[1], and Diego G. Loyola[4]

[1] NASA Goddard Space Flight Center, Greenbelt, MD, 20771, USA
[2] Universities Space Research Association USRA/GESTAR, Columbia, MD, USA
[3] Science Systems and Applications Inc., Lanham, MD USA
[4] German Aerospace Center (DLR), Remote Sensing Technology Institute, Oberpfaffenhofen, 82234 Weßling, Germany
Correspondence to Omar Torres (omar.o.torres@nasa.gov)

Abstract. TROPOMI near-UV radiances are used as input to an inversion algorithm that simultaneously retrieves aerosol optical depth (AOD) and single scattering albedo (SSA) as well as the ~~improved~~ qualitative UV Aerosol Index (UVAI~~) that accurately accounts for the angular scattering effects of water clouds.~~). We first present the TROPOMI aerosol algorithm (TropOMAER), an adaptation of the currently operational OMI near-UV (OMAERUV & OMACA) inversion schemes, that ~~take~~takes advantage of TROPOMI's unprecedented fine spatial resolution at UV wavelengths, and the availability of ancillary aerosol-related information to derive aerosol loading in cloud-free and above-cloud aerosols scenes. ~~An evaluation analysis of~~ TROPOMI-retrieved AOD and SSA products ~~using~~ are evaluated by direct comparison to sun-photometer ~~observations shows~~measurements. A parallel evaluation analysis of OMAERUV and TropOMAER aerosol products is carried out to separately identify the effect of improved instrument capabilities and algorithm upgrades. Results show TropOMAER improved levels of agreement with respect to those obtained with the heritage coarser ~~–~~resolution sensor. OMI and TROPOMI aerosol products are also inter-compared at regional daily and monthly temporal scales, as well as globally at monthly and seasonal scales. We then use TropOMAER aerosol retrieval results to discuss the US Northwest and British Columbia 2018 wildfire season, the 2019 biomass burning season in the Amazon Basin, and the unprecedented January 2020 fire season in Australia that injected huge amounts of carbonaceous aerosols in the stratosphere.

1 Introduction

The TROPOspheric Monitoring Instrument (TROPOMI) on the Sentinel-5 Precursor (S5P) satellite launched on October 13, 2017 is the first atmospheric monitoring mission within the European Union Copernicus program. The objective of the mission is the operational monitoring of trace gas concentrations for atmospheric chemistry and climate applications. TROPOMI is the follow-on mission to the successful Aura Ozone Monitoring Instrument (OMI, Levelt et al., 2006) that has been operating since October 2004, the Global Ozone Monitoring Experiment-2 (GOME-2, Munro et al., 2016) sensors on the Metop (Meteorological Operational Satellite Program of Europe) satellites operating since 2006, and previous missions such as SCanning **I**maging Absorption SpectroMeter for

Atmospheric CHartographY (SCIAMACHY, Bovensmann et al., 1999). The S5P mission precedes the upcoming Sentinel-5 (S5~~) mission,~~), a TROPOMI-like sensor, and the geostationary Sentinel-4 (S4) ~~mission~~missions (Ingmann et al., 2012).

TROPOMI is a high spectral resolution spectrometer covering eight spectral windows from the ultraviolet (UV) to the shortwave infrared (SWIR) regions of the electromagnetic spectrum. The instrument operates in a push-broom configuration, with a swath width of about 2600 km on the Earth's surface. The typical pixel size (near nadir) is 5.5x3.5 km^2 for all spectral bands, with the exception of the UV1 ~~band~~ (5.5x28 km^2) and SWIR ~~bands~~ (5.5x7 km^2~~).~~) bands. On ~~ESA's~~ behalf~~,~~ of the European Space Agency (ESA), the German Aerospace Center (DLR, Deutsches Zentrum für Luft- und Raumfahrt) generates Level 1b calibrated radiance data and level 2 derived products including trace gas (O_3, NO_2, SO_2, CO, CH_4, and CH_2O), aerosols (UV aerosol index ~~and~~, UVAI), O_2-A band aerosol layer height~~)~~ (ALH)) and cloud properties. ~~No~~Currently, no ESA-produced standard quantitative aerosol products are ~~currently~~ available from TROPOMI. Per established NASA~~-~~ (National Aeronautics and Space Administration)-ESA interagency collaboration agreement, TROPOMI level 1b calibrated radiance data and level-2 retrieved products, are available at the Goddard Earth Sciences Data and Information Services Center (GES DISC, ~~https://disc.gsfc.nasa.gov/datasets/).~~https://disc.gsfc.nasa.gov/datasets/).

In this paper, we report the first results of a NASA research aerosol algorithm using TROPOMI observations at near-UV wavelengths. TROPOMI aerosol observations will further extend the multi-decadal long near UV aerosol record started with the Total Ozone Mapping Spectrometer (TOMS) series of sensors (1978-1992; 1996-2001, Torres et al., 1998) and continued into the new millennium by the currently operational OMI instrument (Torres et al., 2007). A similar multi-year AOD/SSA record is also available from EPIC (Earth Panchromatic Imaging Camera) on the DSCOVR (Deep Space Climate Observatory) parked at Lagrange point 1 (Marshak et al., 2018; Ahn et al., 2020).

A description of the algorithm is presented in section 2, followed by a detailed evaluation of retrieval results in section3. In section 4, we use TROPOMI derived information to discuss synoptic~~-~~scale aerosol events ~~taken place~~ in different regions of the world since the launch of TROPOMI in 2017.

Formatted: English (United States)

2 NASA TROPOMI Aerosol Products

2.1 Heritage Algorithm

The NASA OMI aerosol retrieval algorithms for cloud~~-~~free conditions (OMAERUV, Torres et al., 2007; 2013; 2018), and for above-cloud aerosols (OMACA, Torres et al~~.~~,, 2012; Jethva et al., 2018) have been combined into a single algorithm (TropOMAER) and applied to TROPOMI observations. TropOMAER ~~ingests measured TROPOMI radiances~~uses observations at ~~354 nm~~two near-UV wavelengths to calculate the UVAI, and ~~388 nm~~ to retrieve total column aerosol optical depth (AOD) and single scattering albedo (SSA~~)~~). Although detailed documentation of the heritage algorithm is available in the published literature, a brief description is presented here

for ~~cloud-free conditions, and above-cloud aerosol optical depth (ACAOD) for overcast conditions. Retrievals are carried out at 388 nm and reported also at 354 nm and 500 nm~~completeness.

~~TropOMAER also produces an improved~~

2.1.1 UV Aerosol Index ~~(~~

TropOMAER ingests measured TROPOMI radiances at 354 nm and 388 nm to calculate the UVAI~~)~~, a parameter that ~~accurately~~allows distinguishing UV absorbing particles (carbonaceous and desert dust aerosols, volcanic ash) from non-absorbing particles (Herman et al., 1997; Torres et al., 1998). It is defined as,

$$UVAI = -100log_{10}[I_{354}^{obs}/I_{354}^{cal}] \quad (1),$$

where *I* represent the observed and calculated radiances at 354 nm. Measurements at 388 nm are used to obtain a wavelength-independent cloud-fraction that is required for the calculation of the I_{354}^{cal} term (Torres et al., 2018). UVAI yields positive values in the presence of absorbing particles, near-zero for clouds, and small negative values for non-absorbing aerosols.

The magnitude of the aerosol UVAI signal depends mainly on AOD, ALH, and aerosol absorption exponent (AAE). For instance, as shown in Figure 1, for the OMI carbonaceous aerosol model [Torres et al. 2013], and an AAE of 4.8 (i.e., imaginary component of refractive index at 340 nm about 70% higher than at 388 nm), the UVAI increases rapidly with AOD and ALH up to AOD of about 4, at which point the sensitivity to AOD goes down rapidly. For AOD's larger than 6, the UVAI saturates as aerosol absorption of Rayleigh scattered photons peaks, and further UVAI enhancements are only possible for increased values of ALH and/or enhanced aerosol absorption exponent (AAE). Thus, for AOD values larger than about 6, the UVAI effectively becomes a measure of ALH. Although most tropospheric aerosol events fall on the lower left section of Fig. 1 (AOD as large as 4.0 and UVAI as large as 8), observed cases of extraordinarily large UVAI values are generally associated with the injection of huge amounts of UV-absorbing aerosol particles in the upper-troposphere-lower-stratosphere (UTLS) such as ash layers in the aftermath of volcanic eruptions (Krotkov et al., 1999), or wildfire-triggered pyro-cumulonimbus (pyroCb's) episodes (Torres et al., 2020).

The UVAI also contains non-aerosol related information such as ocean color and wavelength-dependent land surface reflectance. It is calculated over the oceans and the continents for all cloud conditions and over ice/snow covered surfaces. TropOMAER UVAI explicitly accounts for the angular scattering effects of water clouds ~~and thus, reduces~~. By doing so the UVAI across-track angular dependence is reduced and ~~eliminates~~ spurious non-zero values, produced by the previously used representation of clouds as opaque Lambert Equivalent Reflectors (LER~~-~~, Torres et al., 2018), are largely eliminated.

2.1.2 Aerosol Algorithm for cloud-free conditions

TROPOMI measured radiances at 354 nm and 388 nm are input to a two-channel inversion algorithm that simultaneously retrieves AOD and SSA for cloud-free conditions (Torres et al., 2007; 2013). Pre-calculated look-up tables (LUTs) of top-of-atmosphere reflectances for pre-defined aerosol types, with nodal points on AOD, SSA and

Formatted: Font: Italic

ALH, surface reflectance, and viewing geometry, are used in the inversion process. Ancillary information on surface albedo ALH, and surface type (Torres et al., 2013) is required.

In the inversion algorithm, it is assumed that for each pixel, the aerosol load can be uniquely represented by one of three types: carbonaceous, desert dust or sulfate particles. Each aerosol type is associated with assumed bi-modal particle size distributions and real component of refractive index (Torres et al., 2007; Jethva and Torres, 2011). Carbonaceous and sulfate particles are assumed to be spherical whereas desert dust aerosols are modelled as non-spherical particles (Torres et al., 2018). UV-absorbing aerosol types are easily differentiated from the non-absorbing kind based ~~UVAI definition (Torres et al., 2018).~~

on UVAI interpretation. As in the heritage ~~OMAERUV~~ algorithm, ~~AIRS~~ observations of carbon monoxide (CO~~),~~) by AIRS (Atmospheric Infrared Sounder) on the Aqua satellite, are used as a tracer of carbonaceous aerosols to separate them from desert dust particles (Torres et al., 2013~~), and~~).

Because of the known sensitivity of satellite measured UV radiances emanating from UV-absorbing aerosols to ALH (Torres et al., 1998), aerosol layer altitude is prescribed using a combination of a CALIOP- (Cloud-Aerosol Lidar with Orthogonal Polarization)-based monthly ALH climatology ~~of aerosol layer height~~and transport model calculations (Torres et al~~.,~~, 2013~~), are used~~).

For each cloud-free, fully characterized pixel in ~~TropOMAER for~~terms of satellite viewing geometry, surface albedo and type, ALH, and aerosol type, a set of AOD and SSA (388 nm) values is extracted from the LUTs by direct matching to the measured radiances. The aerosol ~~type identification and~~ absorption optical depth (AAOD), given by the product of AOD and the single scattering co-albedo (1-SSA), is also reported. In addition to the nominal 388 nm wavelength, parameters are also reported at 354 and 500 nm using the assumed extinction and absorption spectral dependence of the pre-defined aerosol ~~layer height (ALH) determination.~~ models.

Future algorithm ~~enhancement~~enhancements will explore the utilization of TROPOMI retrieved information on ALH and CO, as well as ~~additional~~the additionally available spectral measurements for aerosol typing.

~~TropOMAER uses the ESA-produced VIIRS/SNPP cloud mask re-gridded to the TROPOMI spatial resolution (Siddans, 2016) product for the identification of TROPOMI pixels suitable for aerosol retrieval.~~

Retrievals are carried out over all ice/snow-free land surface types. Over the oceans, retrievals are made only for pixels characterized by UVAI larger than about 1.0, indicating the clear presence of absorbing aerosols in the atmospheric column. No attempt is made to retrieve properties of weakly absorbing or non-absorbing aerosols over the ocean because of the difficulty in separating the atmospheric aerosol signal from that of ocean color. TropOMAER uses an ESA-produced cloud mask based on sub-kilometer resolution radiance measurements at 1.385 μm by NOAA (National Oceanic and Atmospheric Administration)'s Visible Infrared Imaging Radiometer Suite (VIIRS) on the S-NPP (Suomi-National Polar-orbiting Partnership) platform, re-gridded to the TROPOMI spatial resolution (Siddans, 2016). On March 7, 2020 (TROPOMI orbit 12432), the initial NOAA VIIRS cloud mask used with TROPOMI was replaced with the NOAA Enterprise Cloud Mask (ECM) product. The availability of this product, that facilitates the identification of TROPOMI pixels suitable for aerosol AOD/SSA retrieval, is the only algorithmic improvement of TropOMAER in relation to OMAERUV. The heritage algorithm uses thresholds in

measured reflectance, UVAI, and aerosol type [Torres et al., 2013] to identify minimally cloud-contaminated pixels for aerosol retrieval.

2.1.3 Retrieval of above-cloud aerosol optical depth.

When absorbing aerosol are present above clouds in overcast conditions, TROPOMI observations at 354 and 388 nm are used to simultaneously retrieve above cloud aerosol optical depth (ACAOD) of carbonaceous or desert aerosols, as well as the optical depth of the underlying cloud (COD) corrected for aerosol absorption effects Torres et al., 2014).

The algorithmic approach is similar to that of the cloud-free case, except that the retrieved two parameters are ACAOD and COD. Information on single scattering albedo is currently prescribed using an OMI-based long-term SSA climatology (Jethva et al., 2018). The steps involved in aerosol type selection and ALH determination are the same as in the cloud-free retrieval algorithm. A detailed description of the algorithm physical basis and derived products is given in Torres et al. (2014) and Jethva et al., (2018).

2.2 Calibration

In this work, we use the ~~UVIS~~UV-VIS (UV/Visible) band 3 of TROPOMI level 1b product (Kleipool et al., 2018). TROPOMI version 1 reflectances for band 3 are within 5%-10% compared with OMI and OMPS (Rozemeijer and Kleipool, 2019). It is expected that the upcoming version 2 of the TROPOMI level 1b product will solve inconsistencies of the radiometric calibration detected in the UV and UVVIS spectrometers using in-flight measurements and it will include degradation correction for the affected bands (Ludewig et al., 2020).

For this application, we use TROPOMI ~~calibration~~correction coefficients at 354 and 388 nm derived using an ice reflectance based vicarious approach that has been ~~historically~~ used ~~in~~to evaluate the ~~monitoring of~~ calibration of ~~NASA~~ UV-VIS sensors (Jaross and Warner, 2008). ~~A fixed irradiance file was used for the Earth-Sun distance correction. We plan to redo all calibration adjustment and reprocessing when an improved version 2 of the level 1b product is released by ESA.~~

TROPOMI measured reflectances over Antarctica on 28 and 29 November 2017 were compared to radiative transfer model results. We calculate the ratio of each observed across-track ground pixel's reflectance at a specified wavelength to that of the modeled value for the same viewing conditions to obtain an error for that measurement. The model used is exactly the same as was used in the generation of OMI Collection 3 level 1b data (Dobber et al., 2008). The static corrections applied to TROPOMI reflectances elsewhere on the globe were derived by first averaging over all measurement errors at a given across-track position, then further smoothing with a 5-pixel boxcar in the across-track direction. Corrections range from -4% to +2% in the across-track direction for the two wavelengths. We plan to repeat the calibration adjustments and to reprocess when an improved version 2 of the level 1b product is released by ESA.

3 Evaluation ~~of~~ TropOMAER ~~Products~~Performance

Formatted: Space After: 0 pt

~~Evaluation results of TROPOMI retrieved~~ Improved performance of the TropOMAER algorithm in relation to the OMI heritage algorithm is expected as a consequence of both instrumental and algorithmic enhancements. TROPOMI 5.5x3.5 km^2 spatial resolution represents a factor of 16 improvement in relation to OMI's 13x24 km. In addition to its finer nadir resolution, TROPOMI's extreme off-nadir resolution does not increase as much as OMI's. As discussed in section 2.1, the TROPOMI-dedicated VIIRS cloud mask is the only algorithmic improvement in the current version of TropOMAER.

In this section, we evaluate TropOMAER UVAI product in relation to its OMAERUV predecessor, and also compare it to the operational ESA/KNMI (Koninklijk Nederlands Meteorogisch Instituut) TROPOMI UVAI product (Stein, 2018). We also evaluate the accuracy of TROPOMI quantitative AOD and SSA ~~albedo~~aerosol products by comparison to ground-based independent observations. TROPOMI derived aerosol parameters are also compared to OMI results during the same time and similar regions.

3.1 UV Aerosol Index Evaluation

Two consecutive orbit views by OMI and TROPOMI of the smoke plume from the Pacific Northwest fires on August 18, 2018 are shown in Figure 2. OMI's depiction of this event appears in Fig. 2a whereas Fig. 2b illustrates the same aerosol feature as reported by the TropOMAER algorithm. Both products cover a similar range of UVAI values from a slightly negative background to values as high as 10. OMI's coarse spatial resolution, however, is in stark contrast to TROPOMI's fine resolution that allows the mapping of the smoke plume UVAI signal with unprecedented level of detail. Missing data in OMI's depiction in Fig. 2a, is associated with the row anomaly that has reduced the sensor's observing capability by nearly 50% since about 2008 (Torres et al., 2018; Schenkeveld, Jaross at al., 2017). Figure 2c, shows the operational TROPOMI ESA/KNMI UVAI product for the same event. The main difference between the NASA (Fig. 2b) and ESA/KNMI (Fig. 2c) UVAI products is the background values that, while near-zero for the NASA product, reaches values a low as -2 for the KNMI product. The large background difference between the two products is likely the combined effect of calibration uncertainties in the operational ESA/KNMI product, as well as algorithmic differences in the treatment of clouds in the calculated component of the UVAI definition. In the KNMI UVAI calculation, clouds are modelled as opaque reflectors at the ground (Herman et al., 1997), whereas in the NASA UVAI, clouds are explicitly modelled as poly-dispersions of liquid water droplets using ~~ground-based observations are~~ Mie Theory (Torres et al., 2018). A comparative analysis of OMAERUV and TropOMAER UVAI is presented ~~here. A standard~~ in section 3.3.

3.2 Evaluation of retrieved Aerosol Optical Depth and Single Scattering Albedo

We evaluate separately the effect of instrumental and algorithmic improvements in TropOMAER retrieval algorithm by direct comparison of the satellite ~~to ground comparison of measured AOD and SSA was carried out using~~ product to ground-based globally distributed (over land) level 2 Version 3 measurements of ~~these parameters by~~AOD (Giles et al., 2019) by the Aerosol Robotic Network (AERONET, Holben et al., 1998).

~~At~~ Measurements of AOD at 380 nm are available at most AERONET sites ~~AOD at 380 nm is measured~~, allowing a direct comparison to OMI and TROPOMI 388 nm retrievals. ~~However, the AERONET radiance~~No attempt was

made to account for the small AERONET-TROPOMI wavelength difference. AERONET AOD measurements at the twelve sites listed in Table 1 over a two-year period (May-2018 thru May 2020) were used in the analysis. These locations were chosen based on the availability of 380 nm AOD measurements, and on the representativity of environments where most common aerosol types (carbonaceous, desert dust, and sulfate-based) are observed.

3.2.1 Impact of TROPOMI's fine resolution on AOD retrieval

We first analyze the impact of the enhanced spatial resolution by independently comparing OMI retrievals by the OMAERUV algorithm and TropOMAER AOD inversions to AERONET measurements over the selected set of AERONET sites. In this validation exercise, the VIIRS cloud mask is ignored, and the heritage algorithm cloud mask [Torres et al., 2013] is applied to both OMI and TROPOMI observations. Resulting statistics and linear regression fitting parameters for the two validations were compared.

Linear least square regression (LQR) fits are customarily used as a standard method of validating satellite AOD retrievals. The use of this common approach facilitates the relative comparison of the same physical parameter measured by a large variety of sensors and retrieval algorithms. The reported LQR parameters in this manuscript, based on an admittedly small sample of observations, are only intended to illustrate the relative improvement in the accuracy of retrieved parameters associated with TROPOMI enhanced instrumental and algorithmic capabilities with respect to OMI. This is by no means an exhaustive validation exercise of the TROPOMI record for which a lot more AERONET observations are needed.

Ground-based AOD values averaged within ±10 min of the satellite overpass, are compared to spatially averaged retrievals by OMAERUV within a 40 km radius, and by TropOMAER within 20 km (because of the smaller pixel size) of the AERONET site. Figure 3 shows scatter plots of the AERONET-satellite comparisons at the combined 12 sites for OMAERUV (Fig. 3a) and TropOMAER (Fig 3b). The associated statistics and linear regression fitting parameters (y-intercept and slope) are listed in columns 2 and 3 of Table 2. The TROPOMI-AERONET comparison yields 741 matchups compared to OMI's 410, representing an 80% increase. The larger number of coincidences is the result of the combined effect of TROPOMI's finer spatial resolution as well as the OMI's row anomaly (Torres et al., 2018; Schenkeveld, Jaross et al., 2017) affecting OMI since 2007. The TROPOMI results also show an improved correlation coefficient (0.82) with respect to the one (0.60) associated with the OMI observations. The lowest OMAERUV reported correlation coefficients are associated with outlying large AOD estimates resulting from mixtures of UV-absorbing aerosols and clouds, which are difficult to identify at OMAERUV's coarse spatial resolution.

Both comparisons yield about the same slope (0.70), whereas OMI's y-intercept value (0.10) is better than TROPOMI's (0.25). Resulting root mean square errors (rmse) values are 0.31 and 0.19 for OMI and TROPOMI, respectively. Except for the y-intercept, the reported statistics suggest a clear performance improvement of the TROPOMI algorithm directly linked to the sensor's smaller pixel size.

3.2.2 Effect of VIIRS cloud masking on AOD retrieval

The effect of using the VIIRS cloud mask re-gridded to the S5P resolution (Siddans et al., 2016) to identify cloud-free pixels was evaluated by means of a third validation exercise. This time, the TROPOMI-AERONET comparison was carried out for an enhanced TropOMAER algorithm that makes use of the VIIRS dedicated cloud mask. The scatter plot illustrating the outcome of the later comparison is shown in Figure 3c. The corresponding statistical and linear regression parameters are listed in column 4 of Table 2. An inspection of columns 3 and 4, shows that using the VIIRS cloud mask translates into an increase in the number of matchups of over 100 (to 845) as well as higher correlation coefficient (0.89) and slightly improved slope (0.74) and rmse (0.16) values than those reported for the TropOMAER algorithm with heritage cloud mask. The resulting y-intercept is still significantly higher than reported by the OMAERUV-AERONET comparison in column 2, indicating an offset possibly associated with TROPOMI L1 calibration issues.

3.2.3 SSA Evaluation

An analysis similar to that carried out for AOD evaluation is performed for SSA using AERONET Version 3, level 2 inversion product (Sinyuk et al., 2020). The AERONET inversion algorithm that ~~retrieves~~infers aerosol particle size ~~information~~distribution and complex refractive index~~, does not retrieve SSA~~ (from which SSA is calculated) does not include measured sky radiances nor retrieved AOD at wavelengths shorter than 440 nm. Therefore, the evaluation of OMI and TROPOMI retrieved 388 nm SSA ~~retrievals includes the~~requires a wavelength transformation of the satellite products to 440 nm based on the assumed spectral dependence of absorption for each aerosol type in the algorithm (Jethva et al., 2014). ~~Future TROPOMI SSA evaluation work will use measurements from the regional SKYNET network (Nakajima et al., 1996; Hashimoto et al., 2012) that retrieves~~Unlike in the AOD validation, in which the AERONET observation is considered a ground-truth measurement, the AERONET SSA ~~at 380 nm facilitating the direct comparison to satellite measurements (Jethva, et al., 2019).~~product is the result of a remote sensing inversion and, just like the satellite retrievals, subject to non-unique solutions. Thus, the AERONET-satellite SSA analyses discussed here cannot be regarded as a validation of the satellite product, but merely a comparison of the outcome of two independent inversion methods.

~~3.1 AOD Validation~~

~~AOD comparisons at 388 nm were carried out at several AERONET sites. Ground-based AOD values averaged within ±10 min of the satellite overpass, were compared to spatially averaged TROPOMI retrievals within a 20 km radius of the AERONET site. Resulting scatter plots for the 12 representative sites listed in Table 1 are shown in Figure 1. Calculated correlation coefficients and the parameters of the associated linear fit (y-intercept and slope) are summarized in Table 1, along with number of matchups (N) and the percent of matched points in agreement within 30%. The data in Table 1 is listed in decreasing slope value order, to facilitate the discussion.~~

~~The validation exercise yielded correlation coefficients between 0.79 and 0.94 and root mean square error (RMSE) values lower than 0.20 at 10 out of the selected 12 sites. Slightly larger RMSE values (0.22) were obtained at the Lumbini, Nepal and New Delhi, India locations. Regarding the linear fit results, slope values between 0.75 and 1.25~~

~~are reported at 9 sites, and between 0.8 and 1.0 at six sites. The comparison yields y-intercept values between 0.15 and 0.25 at all sites but New Delhi (0.44). The high y-intercept at all sites in this analysis, is likely the result of a remaining calibration offset and/or the effect of the coarse resolution surface albedo data set currently used in TropOMAER. These issues are currently under investigation.~~

~~On surface-satellite AOD scatter plots, the effect of sub-pixel cloud contamination in coarse spatial resolution sensors (TOMS, OMI) shows generally an overestimation at AOD's 0.3 and lower [Torres et al., 2002; Ahn et al., 2014]. In the TROPOMI evaluation discussed here, this effect is apparent at sites associated with typically large aerosol loads (notably Mongu, Banizoumbuo, Beijing). At these sites, subpixel cloud contamination effects are observed in TROPOMI retrieved low AOD values. At sites characterized by lower aerosol burden, however, sub-pixel cloud contamination in TROPOMI AOD retrievals is not as obvious as in similar evaluations of OMI retrievals [Ahn et al., 2014]. This apparent improvement in the quality of satellite near-UV AOD is likely a result of the combined effect of TROPOMI's finer spatial resolution, and the availability of the collocated VIIRS cloud mask that allows the identification of pixels suitable for AOD retrievals with minimum cloud presence.~~

~~3.2 SSA Evaluation~~

~~In the~~Since AERONET's retrieved SSA ~~evaluation, we adopted a spatio-temporal approach to collocate spatially varying~~is accurate within 0.03 for 440 nm AOD ≥ 0.4 (Dubovik et al., 2002, Sinyuk et al., 2020), observations at many sites are required to get meaningful statistics. Thus, OMI and TROPOMI SSA retrievals ~~and temporally varying AERONET SSA inversions. The TROPOMI SSA pixels with quality flag '0' (best) were~~ were averaged in a grid box of size 0.5 deg. x 0.5 deg. centered at the AERONET station~~. On the other hand,~~ at 164 sites. Because the at the near-noon time of the satellite overpass AERONET derived SSA from almucantar scans is considered unreliable (Dubovik et al., 2002), the AERONET Level-2 SSA data were temporally averaged within a ±3 ~~hours of time~~hour window ~~centered at~~from the TROPOMI overpass time~~.~~ under the implicit (and admittedly untested) assumption that SSA does not vary significantly throughout the day. The ~~larger~~chosen six-hour temporal window ~~for AERONET~~ allows early morning and late afternoon inversions that are expected to have better accuracy due to larger solar zenith angle and longer atmospheric path length. ~~The spatially and temporally averaged TROPOMI and AERONET SSA data, respectively, then compared as discussed next.~~Although Version 3 AERONET product has recently introduced hybrid scans aimed at sampling larger air masses covering over wider range scattering angles during the middle of the day, only a fraction of currently deployed sensors is capable of such measurements (Sinyuk et al., 2020).

~~Scatter plots of AERONET (x-axis) and TROPOMI (y-axis) 440 nm SSA are shown in Figure 2 for carbonaceous aerosols (left), desert dust particulate (center), and urban-industrial aerosols (right). About 63% (84%) of matched pairs agree within 0.03(0.05) for carbonaceous aerosols. The levels of agreement are 53% (72%) for desert dust, and 45% (65%) for urban industrial aerosols. Smaller RMSE (0.036) results from the comparison of carbonaceous particles than those of desert dust and urban industrial aerosols that yield RMSE values of 0.041 and 0.048~~

Formatted: Font: Bold

~~respectively. Overall, these results are consistent with previous evaluations of OMI retrievals, showing a better agreement with AERONET for carbonaceous particulate.~~

4

Similarly to the previously described AOD validation exercise, satellite-AERONET SSA comparisons were made by independently applying the heritage cloud screening to OMAERUV retrievals and, both heritage and VIIRS-based cloud masking approaches, to TropOMAER. Figure 4 displays the results of the comparison for different aerosol types. The AERONET-OMI analysis is shown in Fig. 4a, and the result of the AERONET-TROPOMI comparison using heritage cloud screening is displayed in Fig. 4b, whereas the outcome when using the VIIRS cloud mask in the TROPOMI inversion appears in Fig. 4c. A numerical summary of the results is presented in Table 2. In a similar fashion as observed in the AOD retrieval evaluation, the number of coincidences increases from 303 for OMI to 323 for TROPOMI with heritage cloud screening, and to 415 for the TROPOMI/VIIRS cloud mask combination. The reported root-mean-square-difference (rmsd) between the two measurements varies little between the three comparisons. The percent number of retrievals within the stated uncertainty levels is marginally better for OMI than TROPOMI with heritage cloud screening, and significantly better for OMI than TROPOMI with VIIRS cloud mask. A visual inspection of Fig. 4 shows that the satellite retrieved SSA for dust is overestimated for AERONET SSA values lower than about 0.9 in the three comparisons. The observed apparent overestimation of the satellite SSA values for desert dust aerosols (blue symbols) in the OMI comparisons (Figure 4a) has been previously observed and discussed in the literature (Jethva et al., 2014). The apparent overestimation shown in the TROPOMI results (Figs, 4b and 4c) are discernibly larger than seen in the OMI data (Fig 4a). Figs. 4b and 4c also show a clear overestimate in the retrieved SSA of smoke aerosols (red symbols) not seen in the OMI retrievals in Fig. 4a. In general, for all three aerosol types, TROPOMI SSA retrievals are seemingly biased high by 0.01-0.02 compared to those from OMI, suggesting a possible connection with remaining TROPOMI L1 calibration issues.

3.3 OMI-TROPOMI long term continuity

The continuity of the OMI and TROPOMI records of aerosol properties is analyzed in this section. Monthly average values of AOD and AAOD for May 2018 to May 2020 two-year period, calculated for three regions: Eastern United States (EUS) between 25–45◦N and 60– 90◦W; southern Africa (SAF), bounded by 5–25◦S and 15– 35◦E and the Sahara Desert (SAH) zone between 15–30◦N and 30◦E–10◦W. The EUS region is representative of areas predominantly associated with non-absorbing aerosols and clouds. The SAF region is known as an important source area of carbonaceous aerosol-cloud mixtures, whereas the SAH region is the source area of the desert dust part, the most abundant aerosol type.

Figure 5 shows the two-year AOD record produced by the OMAERUV (blue) and TropOMAER (red) algorithms for the three regions. TropOMAER-generated AOD values are consistently higher by about 0.2 than the OMAERUV record for the SAF and SAH regions where the absorbing aerosol load is typically large most of the year. The EUS region shows significantly smaller OMI-TROPOMI differences in monthly mean values. The comparison was also done using a TropOMAER version of the algorithm that uses the heritage cloud screening approach, yielding similar results.

Figure 6 depicts the two-year record in terms of AAOD. Differences as large as 0.03 in the SAH region during the 2018 Spring-Summer months are significantly lower in the 2019 record. Overall, the AAOD time series over the three regions show closer agreement between the two sensors, suggesting a partial cancellation of retrieval errors in SSA and AOD when combined in the AAOD parameter.

Figure 7 shows global three-month (June, July, August 2018) average maps of AAOD from TROPOMI (top) and OMI (bottom) observations. Seasonally occurring features such as the Saharan desert dust signal over Northern Africa and the smoke plumes associated with biomass burning over Namibia, Angola, and Congo are clearly picked by both sensors with comparable AAOD values. Other continental aerosol features such as dust and smoke signal over the western US, and smoke plumes from wildfires in the Norwest Pacific and moving eastward across Canada are detected at similar AAOD values by the two sensors, albeit with a higher level of detail in the TROPOMI product. Similar aerosol signals are also picked up by the two sensors over Saudi Arabia, Norwest India, Pakistan, and Western China. Perhaps, the most striking continental difference in the seasonal map in Fig. 7 is the much larger OMI background AAOD in South America, possibly linked to the difficulty of removing sub-pixel cloud effects at OMI's resolution.

Surprisingly, OMI only shows a very scattered signal of the North Atlantic Saharan dust plume between Northern Africa and the plume's leading edge north of Venezuela over the Caribbean, whereas the TROPOMI product shows an almost continuous North Atlantic plume. In spite of the geographically sparse nature of the OMI AAOD data, there is high consistency in the retrieved values by the two sensors. A similar but less severe difference is also observed over the South Atlantic, where the OMI retrieved carbonaceous aerosol plume is more disperse than what is shown in the TROPOMI map. The combined effect of prevailing sub-pixel cloud contamination and OMI's row anomaly explains the spatially scattered OMI retrievals over the oceans.

Clearly, the full TROPOMI coverage at much higher spatial resolution than OMI and the high-resolution VIIRS cloud mask contribute to a significantly improved near UV aerosol product.

The OMI and TROPOMI gridded 2018 monthly data used to produce the seasonal average maps discussed above are also displayed in Figure 8 as density AAOD (left) and UVAI (right) plots. Although small offsets in UVAI (~0.2) and AAOD (~0.02) between the sensors are apparent, a high degree of correlation between the observations by the two instruments is clearly observed.

4 TROPOMI view of Important Aerosol Events

In this section, we briefly discuss three major continental scale aerosol events that took place during the two-year period following the operational implementation of the S5P mission. The discussed cases include the occurrence of wildfire plumes in both hemispheres, while the third one is likely associated with agricultural practices involving biomass burning in the Amazon region.

4.1 2018 Fire Season in Northwest USA and Canadian British Columbia

The 2018 fire season in the western USA and Canadian British Columbia territory was one of the most active of the last few years. It ~~was~~is estimated that over 8500 fires were responsible for the burning of ~~ ~~over 0.8 million hectares, which is the largest area burned ever recorded according to California Department of Forestry and Fire Protection (fire.ca.gov) and the National Interagency Fire Center (nfic.gov). From mid-July to August, intense fires in Northern California, including the destructive Carr and Mendocino Complex fires, produced elevated smoke layers that drifted to the east and northeast. In 2018, the British Columbia (~~B. C~~BC) province of Canada encountered its worst fire season on record, surpassing the 2017 record, with more than 2000 wildfires and 1.55 million hectares burned accounting for about 60% of the total burned area in Canada in 2018 (https://www2.gov.bc.ca/gov/content/safety/wildfire-status). Figure ~~3~~9 shows the spatial extent of the smoke plume generated by wildfires in Canadian B.C. and northwestern USA on August 18, in terms of ~~UVAI,~~ AOD, and SSA products from both TROPOMI~~.~~ (top) and OMI (bottom) observations (the corresponding UVAI depiction was shown in Fig. 2). The carbonaceous aerosol layers produced by the fires spread over a huge area covering large regions of USA's Midwest and Central Canada. ~~UVAI values as large at 10 associated with above cloud smoke layers can be seen in the Canadian sector of the plume.~~ The height of the aerosol layer ~~oscillated~~varies between 3 and 5 km according to CALIOP observations~~.~~ (not shown). Although OMI's coarse resolution and row-anomaly related reduced spatial coverage are clearly observable, the retrieved AOD and SSA fields by the two sensors look remarkably similar. TROPOMI and OMI AOD retrievals ~~show AOD~~reach values as high as ~~3~~5.0~~,~~ near the sources, generally consistent with AERONET ground~~-~~based observations that, on this day, reported AOD values as large as 1.5 (412 nm) at the Lake Erie site (41.8ºN, 83.2ºW) and values in excess of 3.0 at the Toronto station (43.8ºN, 79.5ºW). ~~Retrieved~~ SSA values in the range 0.~~88~~85-0.92 ~~prevailed~~are retrieved by both sensors over the extended area. Minimum OMI retrieved SSA (0.85) in the vicinity of a source area, however, is lower by about 0.02 than the corresponding TROPOMI measurement, consistent with the relative OMI-TROPOMI SSA differences reported in Fig. 4.

4.2 Amazon Basin 2019 Fires

Figure ~~4~~10 shows the spatial distribution of the September 2019 average TROPOMI ~~Aerosol Index, Aerosol Optical Depth,~~ UVAI, AOD and ~~Aerosol Absorption Optical Depth~~AAOD over the region between the Equator and 40ºS~~,~~ and between 35ºW and 85ºW. ~~Large aerosol concentrations are observed~~Monthly average AOD values of around 2.0 prevailed over the source areas. The smoke plumes were mobilized downwind towards the southeast reaching highly populated areas, where TROPOMI measured monthly average AOD in the vicinity of 1.0 0.9 are reported. downwind over the southeast

Figure ~~5~~11 shows the time series of monthly average OMI AOD over the region over the last 15 years, ~~and~~along with the overlapping TROPOMI AOD observations over the last two years. Seasonal carbonaceous aerosol concentration over the Amazon Basin associated with intense agriculture-related biomass burning has significantly decreased over the last twelve years since 2008. The OMI record shows a remarkable decrease since 2008 when near record high values were observed (Torres et al., 2010). After consecutive AOD September peaks larger than 2.0, in

the three-year 2005-2007 period, the monthly average AOD over the Amazon basin reduced to values about 0.5. An isolated abrupt increase to larger than 2.0 was again observed in 2010. Since then, the September peak AOD value has remained much lower than 1, except for 2017 and 2019, when September average AOD larger than unity was observed. The 2019 peak AOD value (1.25) was also retrieved by TROPOMI observations.

Although the overall regional average was slighter larger than in the previous year, it was about a third of the 2010 peak value. As a result of the prevailing regional atmospheric dynamics in 2019, carbonaceous aerosols generated by seasonal biomass burning over region up north were transported towards the southeast, reaching large urban centers such as Sao Paulo and Curitiba. This aspect of the 2019 fire season generated, generating a lot of media attention.

4.3 Australia 2019-2020 Fires

The 2019-2020 fire season in Australia resulted in 18.6 million burned hectares, most of them in the New South Wales and Victoria southeastern states (SBS News, 2020). It is estimated tens of people died along with billions of animals that were exterminated, including pre-fire near –extinction species (Readfearn, 2020). The intense fire activity likely triggered a number of pyroCb's (pyro-cumulonimbus)pyroCb clouds over a few days between December 30, 2019 and early January 2020, injected large amounts of carbonaceous aerosols in the Southern Hemisphere Upper Troposphere – Lower Stratosphere (UTLS). (Ohneiser et al., 2020). In this section, we describe TROPOMI observations of these events in terms of UVAI and AOD retrievals. As observed in visible satellite imagery (not shown) most of the UTLS injected carbonaceous aerosol material was initially above clouds. TROPOMI near UV observations were used in conjunction with aerosol layer height from CALIOP observations as input to a modified version of TropOMAERthe TROPOMI aerosol algorithm that handles stratospheric aerosol layers. (TropOMAER-UTLS). The retrieved SSA over clear scenes was then used as input in the retrieval of AOD over cloudy pixels (Torres et al., 2012).by the above-cloud-aerosol module described in section 2.1.3.

TROPOMI retrieved AOD was used to produce an estimate of resulting stratospheric aerosol mass (SAM). The SAM calculation procedure involves the separation of the stratospheric AOD component from the total AOD column measurement, and the use of an extinction-to-mass-conversion approximation. described in Appendix A. This approach was previously applied to EPIC (Earth Panchromatic Imaging Camera) near UV AOD retrievals to calculate the SAM associated with the 2017 British Columbia pyroCb's events (Torres et al., 2020).

The identification of stratospheric aerosols is carried out establishing a theoretical relationship between AOD and UVAI for a hypothetical aerosol layer at the tropopause. for assumed values of ALH and AAE (see discussion in section 2.1). CALIOP provided ALH information and assumed AAE value of 4.8 similar to that in Torres et al (2020) were used as input to TropOMAER-UTLS. AOD retrievals associated with UVAI values larger than those indicated by the AOD-UVAI relationship are assumed to correspond to stratospheric aerosols.

Figure 6 illustrates the stratospheric aerosol identification method applied to the carbonaceous aerosol layers resulting from the 2017 British Columbia Fires (Torres et al., 2020) on the left and, on the right, from the 2020 Australia fires. The solid line illustrates the reference AOD-UVAI relationship.at the tropopause height are assumed

to correspond to stratospheric aerosols. Figure 12 shows TROPOMI observed UVAI (y-axis) and retrieved AOD (x-axis) for CALIOP-reported ALH on December 31, 2019. Data points in red indicate retrieval lying above the estimated tropopause height (12 km), while the blue points show retrievals at heights below that level. The altitude locations of the retrievals in relation to the tropopause are determined based on unique viewing-geometry-dependent UVAI-AOD relation for each pixel, difficult to visualize on a single plot. Therefore, a quadratic fit (black line) to all data, i.e., above and below the tropopause, was derived to illustrate, for visualization purposes, the separation of tropospheric and stratospheric aerosols.

Unlike during the 2017 British Columbia fire episodes, when a large fraction of the pyroCb generated aerosol plume remained initially in the troposphere and some of it ascended diabatically to the stratosphere ~~on~~over the next few days (Torres et al., 2020), during the Australian 2020 pyro-convective fires most of the produced carbonaceous aerosols appear to have gone directly into the stratosphere. Figure ~~7~~13 shows TROPOMI retrieved UVAI and AOD fields (total column and stratospheric component) on January 2, 2020. Only small differences in the total column and above-tropopause AOD fields are observed, as most of the aerosol material was directly deposited in the stratosphere.

Stratospheric AOD values were converted to mass estimates using the procedure described in Torres et al. (2020) and also included as Appendix ~~1 for completeness.~~A in this paper. Figure ~~8~~14 shows calculated daily values of aerosol mass (in kilotons) from December 31, 2019 thru January 7, 2020, resulting from aerosols above 12 km, altitude used as a proxy of the tropopause height. Separate aerosol mass retrievals were carried out for cloud ~~-~~free (blue bars) and cloudy scenes~~,~~ (green bars), with the daily total SAM given as the sum of these two components~~.~~ (orange bars). The observed daily monotonic increase from 119 kt on December 31, 2019 to 380 kt on January 2, 2020 is likely the result of distinct pyroCb events that seemingly injected most of the aerosol mass directly in the stratosphere. Following the January 2 maximum, SAM decreases over the following three days to a minimum of 87 kt on January 5, as a result of dilution processes, than spreads the aerosol layer horizontally and thins it out~~, so that the sensitivity of total mappers is significantly reduced.~~. The sudden increase to 166 kt on January 6 is ~~possibly~~likely associated with another pyroCb event observed on January 4 that injects an additional 166 kt. Thus, the TROPOMI-based total SAM estimate is the sum of the two peaks on January 2 and January 6 yielding a total of 546 kt, which about twice as much as the 268 kt estimated SAM for the 2017 British Columbia pyroCb ~~that yielded 268 kt~~ [Torres et al., 2020~~].~~] using the same mass estimation technique. The uncertainty of the estimated SAM is ±40~~%~~%, which represents the combined effect of uncertainties on assumed ~~aerosol layer height~~AAE (±0.5) in the AOD retrieval, and the uncertainty ~~in~~associated with the assumed aerosol density ~~(Appendix~~range of 0.79 and 1.53 g-cm−3 (Reid et al., 2005).

5 Summary and future work

The NASA TropOMAER aerosol algorithm applied to TROPOMI observations is ~~a modified~~an adapted version of the ~~one applied to~~ OMAERUV algorithm developed for OMI ~~observations.~~. Currently, the only algorithm upgrade of TropOMAER is the use of a dedicated VIIRS-based cloud mask. Initial retrieval results for the first two years of

operation of the TROPOMI sensor were reported. ~~Standard evaluation procedures using ground-based observations were carried out~~

Since radiometric calibration uncertainties in the range 5-10%, relative to OMI and S-NPP OMPS measurements, are reportedly present the TROPOMI version 1 level1b UVVIS (UV/Visible) band 3 (Rozemeijer and Kleipool, 2019), we applied vicariously derived correction factors to TROPOMI measured radiances at 354 and 388 nm. The approach, based on measured ice reflectances and radiative transfer calculations, yield corrections in the range from -4% to +2% in the across-track direction for both wavelengths.

The AERONET Version 3, level 2 380 nm AOD data record was used to evaluate the ~~accuracy of TropOMAER~~ performance of the TropOMAER algorithm. An AERONET AOD data aggregate consisting of two years (May 2018-May 2020) of observations at 12 sites representative of most commonly aerosol types (i.e., carbonaceous, desert dust, and urban-industrial aerosols) was used in the analysis. To separately evaluate the effects of instrumental and algorithmic improvements on retrieved products, we carried out a three-way comparison of satellite retrieved AOD to AERONET observations: 1) OMI retrievals ~~of AOD and SSA at 388 nm. Satellite~~by the OMAERUV algorithm, 2) TropOMAER retrievals ~~of AOD were~~ using the heritage (OMAERUV) cloud screening method, and 3) TropOMAER retrievals using a VIIRS-based cloud mask were independently compared ~~to AERONET observations at 12 locations representative of where carbonaceous aerosols and urban industrial aerosol types are typically present. The~~ to AERONET observations. A comparative analysis of evaluations 1 and 2 shows the impact of enhanced instrumental capabilities, whereas the analysis of evaluations 2 and 3 highlights the effect of using the VIIRS cloud mask, which is the only TropOMAER algorithmic modification.

The comparison of the linear fit statistics resulting from comparisons 1 and 2 indicate that a large increase in the number of matched observations (from 410 to 741) and higher correlation coefficient (from 0.60 to 0.82) are the main benefit of TROPOMI's enhanced resolution. Resulting slopes and rmse values are similar for both comparisons. However, the AERONET-TropOMAER (with heritage cloud mask) comparison yields a y-intercept value (0.25) more than twice that of the AERONET-OMAERUV analysis (0.10). The comparison of evaluations 2 and 3, intended to identify the contribution of the available VIIRS cloud mask, shows further improvements in the number of matched pairs (from 741 to 845) and correlation coefficient (from 0.82 to 0.89). The other metrics are very similar, including the large y-intercept. A similar analysis using observations at 164 sites was carried out to evaluate TROPOMI's SSA product yielding the similar main conclusion of increased number or retrieval opportunities for the higher spatial resolution sensor.

The expected improvement associated with TROPOMI's higher spatial resolution appears exacerbated in view of the row anomaly affecting the OMI sensor that has reduced by nearly 50% its viewing capability. The TropOMAER higher than OMI y-intercept when compared to AERONET, suggests that a small radiometric calibration offset remains on the corrected TROPOMI measured reflectances used in this analysis.

The TropOMAER aerosol products were also evaluated by direct comparison to OMI at daily, monthly, and seasonal temporal scales. A comparative analysis OMI and TROPOMI two-year time series of AOD monthly values shows that TROPOMI AOD values are higher than OMI by about 0.2. This AOD offset is of about the same

magnitude as identified in the validation ~~exercise yielded correlation coefficients between 0.79 and 0.94 and rms values better than 0.20 at 10 out if the 12 sites. Linear fit results~~analysis using AERONET observation.

Although TROPOMI products show ~~slope values between 0.75 and 1.25 at 9 sites, and between 0.8 and 1.0~~improved spatial coverage especially over the oceans where clouds are a significant obstacle at ~~six locations. Reported y-intercept values vary between 0.15 and 0.25 at all sites but New Delhi (0.44). These generally high values are likely due to remaining calibration offsets and/or the effect of the currently used~~ OMI's coarse resolution ~~surface albedo data. The initial AERONET-TropOMAER SSA evaluation indicates that nearly 63% (84%) of matched pairs agree within 0.03(0.05) for carbonaceous aerosols, 53% (72%) for desert dust, and 45% (65%) for urban industrial aerosols. These levels of agreement are similar to previous~~, the reported ~~evaluation analyses of OMI aerosol retrievals~~comparisons show an overall consistent picture that allows for the long-term continuity of the near-UV aerosol record.

Three ~~important~~continental-scale carbonaceous aerosol events ~~that~~over the last two years captured the attention of climate scientists and news media alike. These events, observed by TROPOMI, were briefly described here in terms of TropOMAER products.

The atmospheric aerosol load generated by the hundreds of fires in the western USA and Southern Canada in the summer of 2018 was measured by both ground-based and spaceborne sensors. The fires-triggered aerosol layers extended over a huge area covering large regions of the USA's Midwest and Central Canada. Except for the difference in spatial resolution, OMI and TROPOMI observations yield a consistent view of this event with UVAI values as large as 10 produced ~~by above cloud smoke layers were frequently observed. According to CALIOP observations the height of the aerosol layers oscillated between 3 and 5 km. TROMOPI AOD retrievals show~~and retrieved AOD values as high as ~~3~~5.0, consistent with AERONET ground based observations at several sites.

After eight years of noticeable reduced biomass burning in Southern Brazil during August and September, ~~a period when agriculture-related biomass burning takes place, numerous fires and, therefore,~~ high levels of carbonaceous aerosols presence were detected in 2019 by both OMI and TROPOMI. As a result of prevailing regional atmospheric dynamics in 2019, carbonaceous aerosols generated by seasonal biomass burning were transported towards the southeast reaching large urban centers. OMI and TROPOMI reported September 2019 monthly and regional average AOD was slightly larger than in the previous year, and about a third of OMI reported 2010 peak (~2.5) value.

A number of pyroCb's likely triggered by intense bushfires in the New South Wales province of Australia between December 30, 2019 and early January 2020 injected large amounts of carbonaceous aerosols in the Southern Hemisphere UTLS. Very large values of TROPOMI UVAI observations pointed to an elevated aerosol layer, which was confirmed by CALIOP reports of a distinct high-altitude aerosol layers near 12 km, above tropospheric clouds. TROPOMI retrieved AOD over both cloud-free and cloudy scenes was used to produce an estimate of the injected aerosol mass above 12 km, yielding a total of 546 kt, which is at least twice as much as the estimated carbonaceous aerosol mass injected in the stratosphere by the 2017 Canadian fires. ~~Unlike during the 2017 British Columbia fire~~

Formatted: Left, Space After: 10 pt

episodes, when pyroCb-generated aerosol plume reached the stratosphere in about three days, the 2020 Australian plume seem to have been directly injected into the lower stratosphere.

Future TropOMAER algorithm enhancement will explore the utilization of TROPOMI retrieved information on aerosol layer height (Nanda et al., 2019), CO (Martínez-Alonso et al., 2020), clouds (Loyola et al., 2018), geometry-dependent effective LER (Loyola et al., 2020), as well as taking advantage of additional available spectral measurements for aerosol typing. Work is currently underway on the development of a higher spatial resolution surface albedo data and on the optimization of the instrument characterization.

References

Ahn, C., Torres, O., Jethva, H., and Tiruchirapalli, R., and Huang, L-K., (2020), Diurnal Variability of Aerosol Properties observed by the DSCOVR/EPIC Instrument from the Earth-Sun Lagrange 1 Orbit, JGR-Atm in review

Ahn, C., O. Torres, and H. Jethva *(*2014*),* Assessment of OMI near-UV aerosol optical depth over land, J. Geophys. Res. Atmos., 119, 2457–2473, *doi:*10.1002/2013JD020188.

Bovensmann, H., Burrows, J. P., Buchwitz, M., Frerick, J., Noël, S., Rozanov, V. V., Chance, K. V., and Goede, A. P. H.: SCIAMACHY: Mission Objectives and Measurement Modes, Journal of the Atmospheric Sciences, 56, 127–150, https://doi.org/10.1175/1520-0469(1999)056%3C0127:SMOAMM%3E2.0.CO;2, 1999.

Dobber, M., Kleipool, Q., Dirksen, R., Levelt, P., Jaross, G.,Taylor, S., Kelly, T., Flynn, L., Leppelmeier, G., and Roze-meijer, N.: Validation of Ozone Monitoring Instrument level1b data products, J. Geophys. Res.-Atmos., 113, D15S06,https://doi.org/10.1029/2007JD008665, 2008.

Gassó, S. and Torres, O.: The role of cloud contamination, aerosol layer height and aerosol model in the assessment of the OMI near-UV retrievals over the ocean, Atmos. Meas. Tech., 9, 3031-3052, doi:10.5194/amt-9-3031-2016, 2016.

Genkova, I., Robaidek, J., Roebling, R., Sneep, M., and Veefkind, P.: Temporal co-registration for TROPOMI cloud clearing, Atmos. Meas. Tech., 5, 595–602, https://doi.org/10.5194/amt-5-595-2012, 2012.

Hashimoto, M., Nakajima, T., Dubovik, O., Campanelli, M., Che, H., Khatri, P., Takamura, T., and Pandithurai, G.: Development of a new data-processing method for SKYNET sky radiometer observations, Atmos. Meas. Tech., 5, 2723–2737, https://doi.org/10.5194/amt-5-2723-2012, 2012

Giles, D. M., Sinyuk, A., Sorokin, M. G., Schafer, J. S., Smirnov, A., Slutsker, I., Eck, T. F., Holben, B. N., Lewis, J. R., Campbell, J. R., Welton, E. J., Korkin, S. V., and Lyapustin, A. I. (2019): Advancements in the Aerosol Robotic Network (AERONET) Version 3 database – automated near-real-time quality control algorithm with improved cloud screening for Sun photometer aerosol optical depth (AOD) measurements, Atmos. Meas. Tech., **12**, 169-209, https://doi.org/10.5194/amt-12-169-2019.

van de Hulst, H. C., Light Scattering by Small Particles, chapter 6, New York, Dover Publications, Inc., 1957.

Ingmann, P., Veihelmann, B., Langen, J., Lamarre, D., Stark, H., and Courrèges-Lacoste, G. B.: Requirements for the GMES Atmosphere Service and ESA's implementation concept: Sentinels-4/-5 and -5p, REMOTE SENS ENVIRON, 120, 58 – 69, https://doi.org/https://doi.org/10.1016/j.rse.2012.01.023, 2012

Jaross, G., and J. Warner (2008), Use of Antarctica for validating reflected solar radiation measured by satellite sensors, J. Geophys. Res., 113, D16S34, doi:10.1029/2007JD008835.

Jethva, H., Torres, O., and Ahn, C.: A 12-year long global record of optical depth of absorbing aerosols above the clouds derived from the OMI/OMACA algorithm, Atmos. Meas. Tech., 11, 5837-5864, https://doi.org/10.5194/amt-11-5837-2018, 2018.

Jethva, H., O. Torres, and C. Ahn (2014), Global assessment of OMI aerosol single-scattering albedo using ground-based AERONET inversion, J. Geophys. Res. Atmos., 119, doi:10.1002/2014JD021672.

Kleipool, Q., Ludewig, A., Babic, L., Bartstra, R., Braak, R., Dierssen, W., Dewitte, P.-J., Kenter, P., Landzaat, R., Leloux, J., Loots, E., Meijering, P., van der Plas, E., Rozemeijer, N., Schepers, D., Schiavini, D., Smeets, J., Vacanti, G., Vonk, F., and Veefkind, P.: Prelaunch calibration results of the TROPOMI payload on-board the Sentinel-5 Precursor satellite, Atmos. Meas. Tech., 11, 6439–6479, https://doi.org/10.5194/amt-11-6439-2018, https://www.atmos-meas-tech.net/11/6439/2018/, 2018.

Krotkov, N.A., O. Torres, C. Seftor, A.J. Krueger, A. Konstinski, W.I. Rose, G.J.S. Bluth, D. Schneider and S.J. Schaefer, Comparison of TOMS and AVHRR Volcanic Ash Retrievals from the August 1992 Eruption of Mt Spurr, *Geophys. Res. Let*., 26, 455-458, 1999

Levelt, P. F., van den Oord, G. H., Dobber, M. R., Malkki, A., Visser, H., de Vries, J., Stammes, P., Lundell, J. O., and Saari, H.: The ozone monitoring instrument, IEEE Transactions on Geoscience and Remote Sensing, 44, 1093–1101, https://doi.org/10.1109/TGRS.2006.872333, 2006.

Loyola, D. G., Xu, J., Heue, K.-P., and Zimmer, W.: Applying FP_ILM to the retrieval of geometry-dependent effective Lambertian equivalent reflectivity (GE_LER) daily maps from UVN satellite measurements, Atmos. Meas. Tech., 13, 985–999, https://doi.org/10.5194/amt-13-985-2020, 2020.

Loyola, D. G., Gimeno García, S., Lutz, R., Argyrouli, A., Romahn, F., Spurr, R. J. D., Pedergnana, M., Doicu, A., Molina García, V., and Schüssler, O.: The operational cloud retrieval algorithms from TROPOMI on board Sentinel-5 Precursor, Atmos. Meas. Tech., 11, 409–427, https://doi.org/10.5194/amt-11-409-2018, 2018.

Ludewig, A., Kleipool, Q., Bartstra, R., Landzaat, R., Leloux, J., Loots, E., Meijering, P., van der Plas, E., Rozemeijer, N., Vonk, F., and Veefkind, P.: In-flight calibration results of the TROPOMI payload on-board theSentinel-5 Precursor satellite, Atmos. Meas. Tech. Discuss., https://doi.org/10.5194/amt-2019-488, in review, 2020.

Marshak, A., J. Herman, S. Adam, B. Karin, S. Carn, A. Cede, I. Geogdzhayev, D. Huang, L. Huang, Y. Knyazikhin, M. Kowalewski, N. Krotkov, A. Lyapustin, R. McPeters, K.G. Meyer, O. Torres, and Y. Yang, 2018: Earth Observations from DSCOVR EPIC Instrument. *Bull. Amer. Meteor. Soc.*, 99, 1829–1850, doi:10.1175/BAMS-D-17-0223.1Martínez-Alonso, S., Deeter, M., Worden, H., Borsdorff, T., Aben, I., Commane, R., Daube, B., Francis, G., George, M., Landgraf, J., Mao, D., McKain, K., and Wofsy, S.: 1.5 years of TROPOMI CO measurements: Comparisons to MOPITT and ATom, Atmos. Meas. Tech. Discuss., https://doi.org/10.5194/amt-2020-63, in review, 2020.Munro, R., Lang, R., Klaes, D., Poli, G., Retscher, C., Lindstrot, R., Huckle, R., Lacan, A., Grzegorski, M., Holdak, A., Kokhanovsky, A., Livschitz, J., and Eisinger, M.: The GOME-2 instrument on the

Metop series of satellites: instrument design, calibration, and level 1 data processing – an overview, Atmos. Meas. Tech., 9, 1279–1301, https://doi.org/10.5194/amt-9-1279-2016, 2016.

Nakajima, T., Tonna, G., Rao, R., Boi, P., Kaufman, Y., and Holben, B.: Use of sky brightness measurements from ground for remote sensing of particulate polydispersions, Appl. Optics, 35, 15, 2672–2686, 1996.

Nanda, S., de Graaf, M., Veefkind, J. P., Sneep, M., ter Linden, M., Sun, J., and Levelt, P. F.: Validating TROPOMI aerosol layer height retrievals with CALIOP data, Atmos. Meas. Tech. Discuss., https://doi.org/10.5194/amt-2019-348, in review, 2019.

Ohneiser, K., Ansmann, A., Baars, H., Seifert, P., Barja, B., Jimenez, C., Radenz, M., Teisseire, A., Floutsi, A., Haarig, M., Foth, A., Chudnovsky, A., Engelmann, R., Zamorano, F., Bühl, J., and Wandinger, U.: Smoke of extreme Australian bushfires observed in the stratosphere over Punta Arenas, Chile, in January 2020: optical thickness, lidar ratios, and depolarization ratios at 355 and 532 nm, Atmos. Chem. Phys., 20, 8003–8015, https://doi.org/10.5194/acp-20-8003-2020, 2020

Readfearn, G., 2020, *Silent death: Australia's bushfires push countless species to extinction"*, Guardian Australia, *3 January 2020*.

Reid, J. S., Koppmann, R., Eck, T. F., and Eleuterio, D. P.: A review of biomass burning emissions part II: intensive physical properties of biomass burning particles, Atmos. Chem. Phys., 5, 799-825, https://doi.org/10.5194/acp-5-799-2005, 2005.

Rozemeijer, N. C. and Kleipool, Q.: S5P Level 1b Product Readme File, S5P-MPC-KNMI-PRF-L1B, available at: https://sentinel.esa.int/web/sentinel/technical-guides/sentinel-5p/products-algorithms and http://www.tropomi.eu/documents/level-0-1b (last access: 26 March 2020), 2019.

SBS News,2020, The numbers behind Australia's catastropic bushfire season, SBS News. 5 January 2020.

Siddans, R., S5P-NPP Cloud Processor ATBD, S5P-NPPCRAL-ATBD-0001, available at: https://sentinel.esa.int/web/sentinel/technical-guides/sentinel-5p/products-algorithms and http://www.tropomi.eu/documents/atbd, (last access: 26 March 2020), 2016

Schenkeveld, V. M. E., Jaross, G., Marchenko, S., Haffner, D., Kleipool, Q. L., Rozemeijer, N. C., Veefkind, J. P., and Levelt, P. F.: In-flight performance of the Ozone Monitoring Instrument, Atmos. Meas. Tech., 10, 1957–1986, https://doi.org/10.5194/amt-10-1957-2017, 2017.

Stein Zweers, D.C., TROPOMI ATBD of the UV aerosol index, S5P-KNMI-L2-0008-RP, available at: https://sentinel.esa.int/web/sentinel/technical-guides/sentinel-5p/products-algorithms and http://www.tropomi.eu/documents/atbd (last access: 11 August 2020), 2018

Sinyuk, A., Holben, B. N., Eck, T. F., Giles, D. M., Slutsker, I., Korkin, S., Schafer, J. S., Smirnov, A., Sorokin, M., and Lyapustin, A.: The AERONET Version 3 aerosol retrieval algorithm, associated uncertainties and comparisons to Version 2, Atmos. Meas. Tech., 13, 3375–3411, https://doi.org/10.5194/amt-13-3375-2020, 2020.

Torres, O., Bhartia, P. K., Taha, G., Jethva, H., Das, S., Colarco, P., et al (2020). Stratospheric Injection of Massive Smoke Plume from Canadian Boreal Fires in 2017 as seen by DSCOVR-EPIC, CALIOP and OMPS-LP Observations. *Journal of Geophysical Research: Atmospheres*, 125, e2020JD032579. https://doi.org/10.1029/2020JD032579

Formatted: Spanish (United States)

Torres, O., Bhartia, P. K., Jethva, H., and Ahn, C.: Impact of the ozone monitoring instrument row anomaly on the long-term record of aerosol products, Atmos. Meas. Tech., 11, 2701-2715, https://doi.org/10.5194/amt-11-2701-2018, 2018.

Torres, O., Ahn, C., and Chen, Z.: Improvements to the OMI near UV aerosol algorithm using A-train CALIOP and AIRS observations, Atmos. Meas. Tech., 6, 3257-3270, doi:10.5194/amt-6-3258-2013, 2013

Torres, O, H. Jethva, and P.K. Bhartia, Retrieval of Aerosol Optical Depth above Clouds from OMI Observations: Sensitivity Analysis and Case Studies, Journal. Atm. Sci., 69, 1037-1053, doi:10.1175/JAS-D-11-0130.1, 2012

Torres, O., A. Tanskanen, B. Veihelman, C. Ahn, R. Braak, P. K. Bhartia, P. Veefkind, and P. Levelt, Aerosols and Surface UV Products from OMI Observations: An Overview, , *J. Geophys. Res.*, 112, D24S47, doi:10.1029/2007JD008809, 2007

Site (country)	Lat., Lon.	N	Corr.coef	y-int	Slope	RMSE	Q30%
Hohenpeissenberg (Germany)	47.8N8°N, 11.0E0°E	78	0.81	0.15	1.21	0.09	17
GSFC (USA)	39.0N0°N, 76.8W8°W	50	0.80	0.19	0.99	0.11	22
Lille (France)	50.6N6°N, 3.1E1°E	47	0.88	0.20	0.97	0.09	17
Beijing-CAMS (China)	39.9N9°N, 116.3E3°E	53	0.94	0.23	0.92	0.18	53
Thessaloniki (Greece)	40.6N6°N, 23.0E0°E	103	0.79	0.19	0.84	0.09	41
Fukuoka (Japan)	33.5N5°N, 130.5E5°E	52	0.84	0.16	0.83	0.10	60
Banizoumbou (Niger)	13.5N5°N, 2.7E7°E	111	0.81	0.23	0.81	0.19	54
Mongu (Zambia)	15.3S3°S, 23.3E3°E	122	0.91	0.25	0.76	0.12	43
Leipzig (Germany)	51.4N,4°N, 12.4E4°E	40	0.81	0.27	0.75	0.11	23
Lumbini (Nepal)	27.5N5°N, 83.3E3°E	67	0.85	0.19	0.69	0.22	73
Yonsei_univUniversity (S. Korea)	37.6N6°N, 126.9E9°E	90	0.85	0.25	0.62	0.14	56
New Delhi (India)	28.6N6°N, 77.2E2°E	42	0.79	0.44	0.59	0.22	76

Table 1: AERONET sites used for the AOD validation analysis presented in this study.

Deleted Cells
Formatted: Font: Bold
Deleted Cells
Deleted Cells
Formatted Table
Deleted Cells
Deleted Cells
Deleted Cells

	OMAERUV	TropOMAER (Heritage Cloud Mask)	TropOMAER (VIIRS Cloud Mask)
Number of matchups	410	741	845
Correlation coefficient	0.62	0.82	0.89
Root Mean Square	0.31	0.19	0.16
Slope	0.70	0.71	0.74
Y-intercept	0.10	0.25	0.24

Table 2. Summary of linear fit results between AERONET measured and ~~TROPOMI~~satellite retrieved AOD at 12 locations~~. Third~~ (column ~~is the~~ 1) by the OMAERUV algorithm (column 2), TropOMAER Heritage algorithm (column 3), and TropOMAER algorithm with VIIRS cloud mask (column 4).

Formatted: Font: Not Bold

Formatted: Font: Not Bold

Formatted: Font: Not Bold

	OMAERUV	TropOMAER (Heritage Cloud Mask)	TropOMAER (VIIRS Cloud Mask)
Number of matchups	303	323	415
Root Mean Square	0.046	0.040	0.044
Percent within 0.03	52	51	48
Percent within 0.05	78	75	70

Table 3. Number of coincidences, root mean square, and percent number of ~~**matchups, columns fourth to six (Q30%)**~~SSA retrievals within 0.03 and 0.05 of AERONET values (column 1) for OMAERUV (column 2), TropOMAER with heritage cloud mask, and TropOMAER with VIIRS cloud mask (column 3).

Formatted: Font: Not Bold

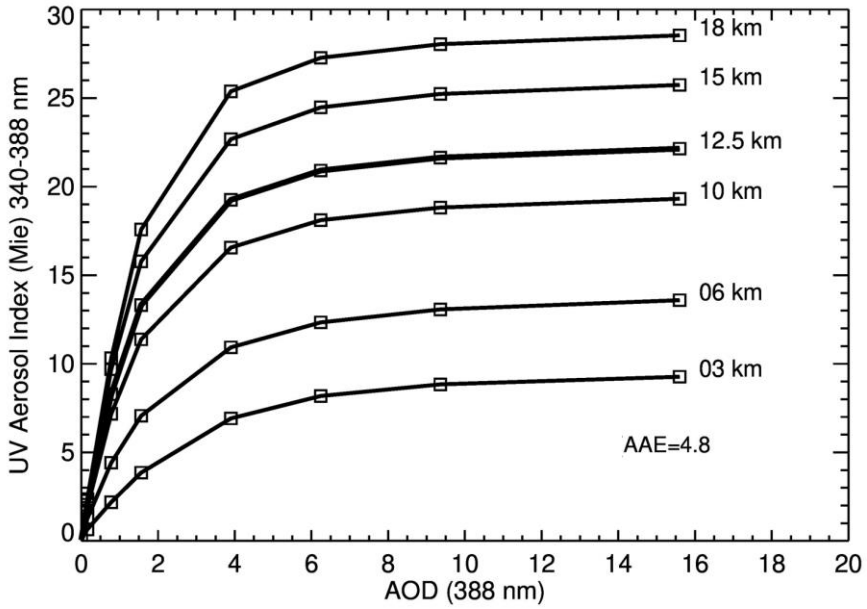

Figure 1. Modelled relationship between UVAI and AOD as a function of ALH for carbonaceous aerosols of assumed 340-388 nm aerosol absorption exponent of 4.8 (see text for details).

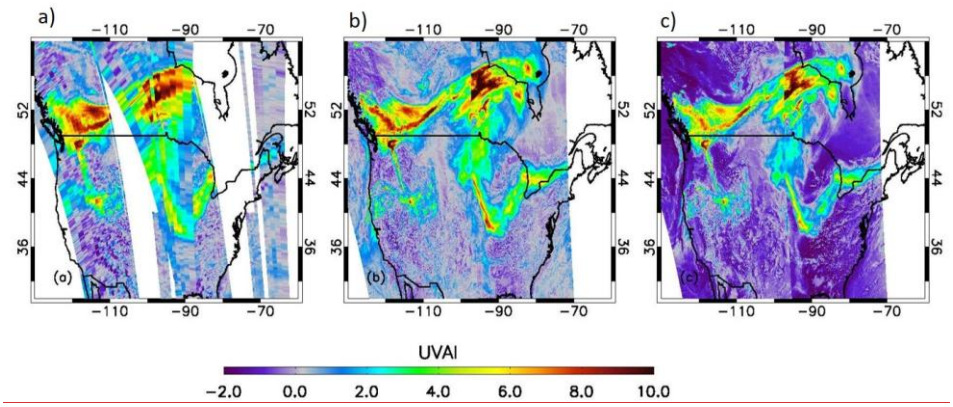

Figure 2. Observed UVAI on August 18, 2018 over North America from a) OMI observations, b) TROPOMI observations using the NASA algorithm and, c) TROPOMI operational ESA/KNMI product.

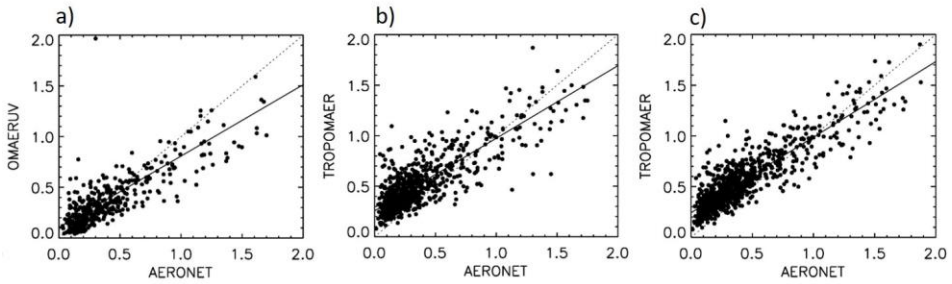

Figure 3. AERONET – satellite comparisons of OMI retrieved AOD (a), TROPOMI using heritage cloud screening (b) TROPOMI using VIIRS cloud mask (c) Dotted line indicates the ~~number of (in percent) retrievals~~ one-to-one line, and solid line is the calculated linear fit. See the text for details.

Formatted: Font: Not Bold

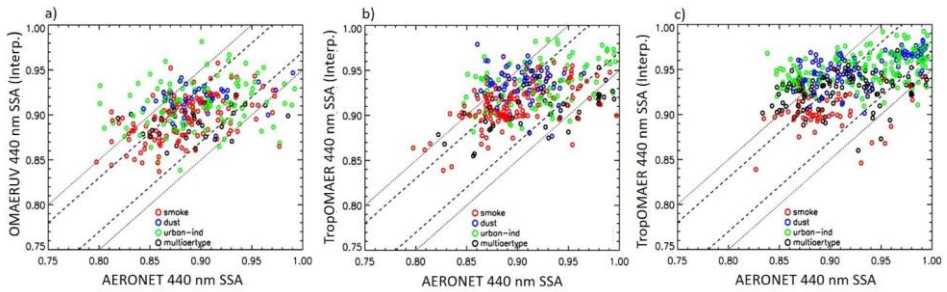

Figure 4. As in Figure 3 for single scattering albedo of dust aerosols (blue), smoke aerosols (red), urban-industrial aerosols (green), and aerosol mixtures (black). Dashed line indicates agreement ~~within 30% with the ground-truth observations.~~

Formatted: Font: 11 pt, Not Bold

Formatted: Font: 11 pt, Not Bold

between ±0.03, solid line indicates agreement between ±0.05.

Formatted: Font: 11 pt, Not Bold

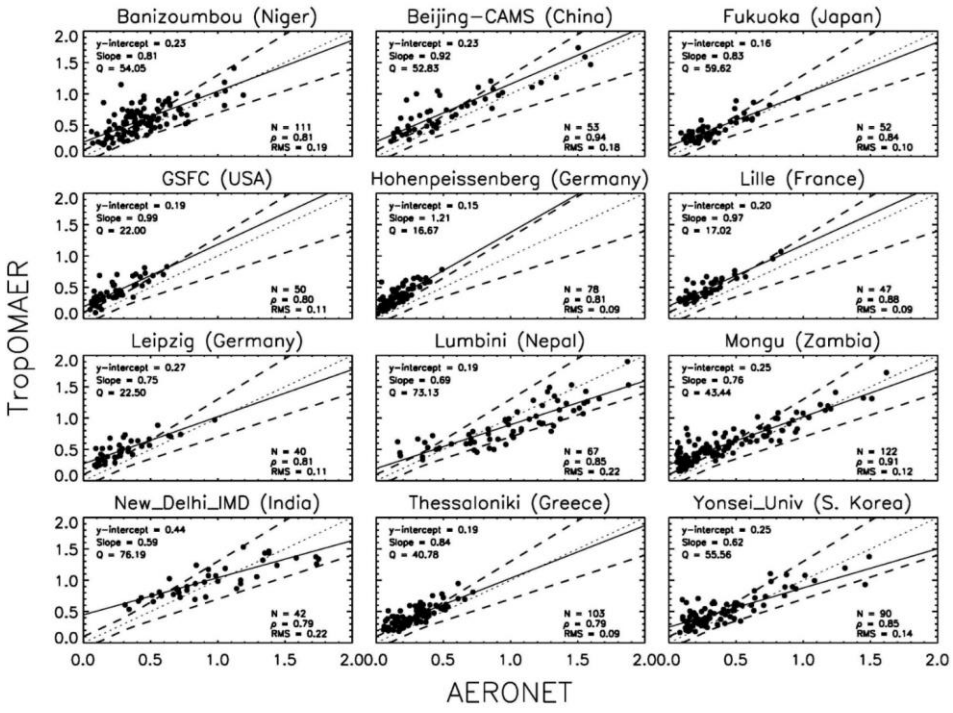

~~Figure 1: Comparison of TROPOMI AOD to AERONET observations at diverse locations around the world.~~

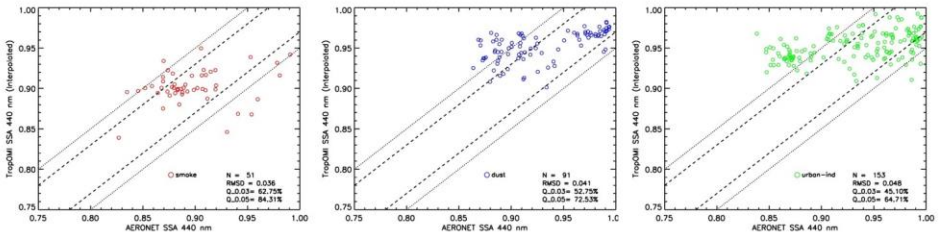
TropOMI SSA 440 nm (Interpolated)
AERONET SSA 440 nm
smoke
N = 51
RMSD = 0.036
Q_0.03= 82.75%
Q_0.05= 84.31%
dust
N = 91
RMSD = 0.041
Q_0.03= 52.75%
Q_0.05= 72.53%
urban-ind
N = 153
RMSD = 0.048
Q_0.03= 45.10%
Q_0.05= 64.71%

1

2

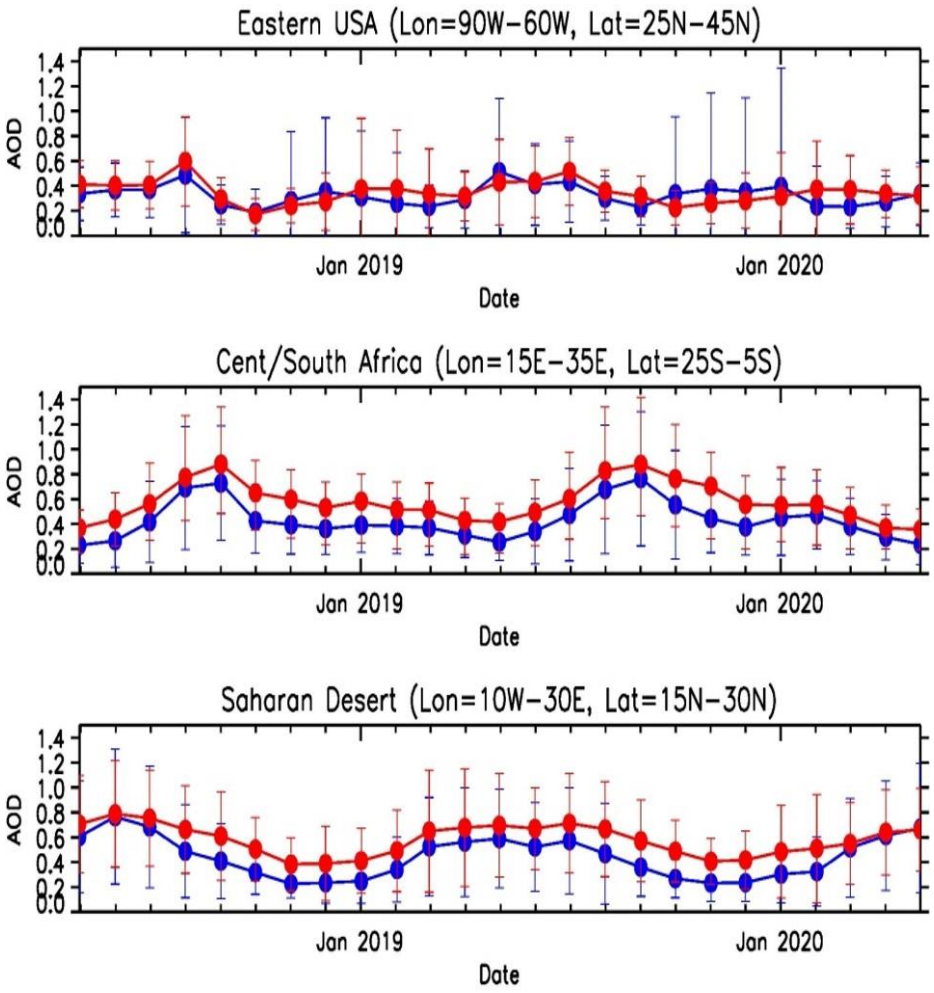

Figure 5. Two-year time series of monthly average OMI (inblue) and TROPOMI (inred) AOD values for Eastern United States (top), Southern Africa (middle), and Saharan Desert (bottom). Vertical lines indicate standard deviation of the mean.

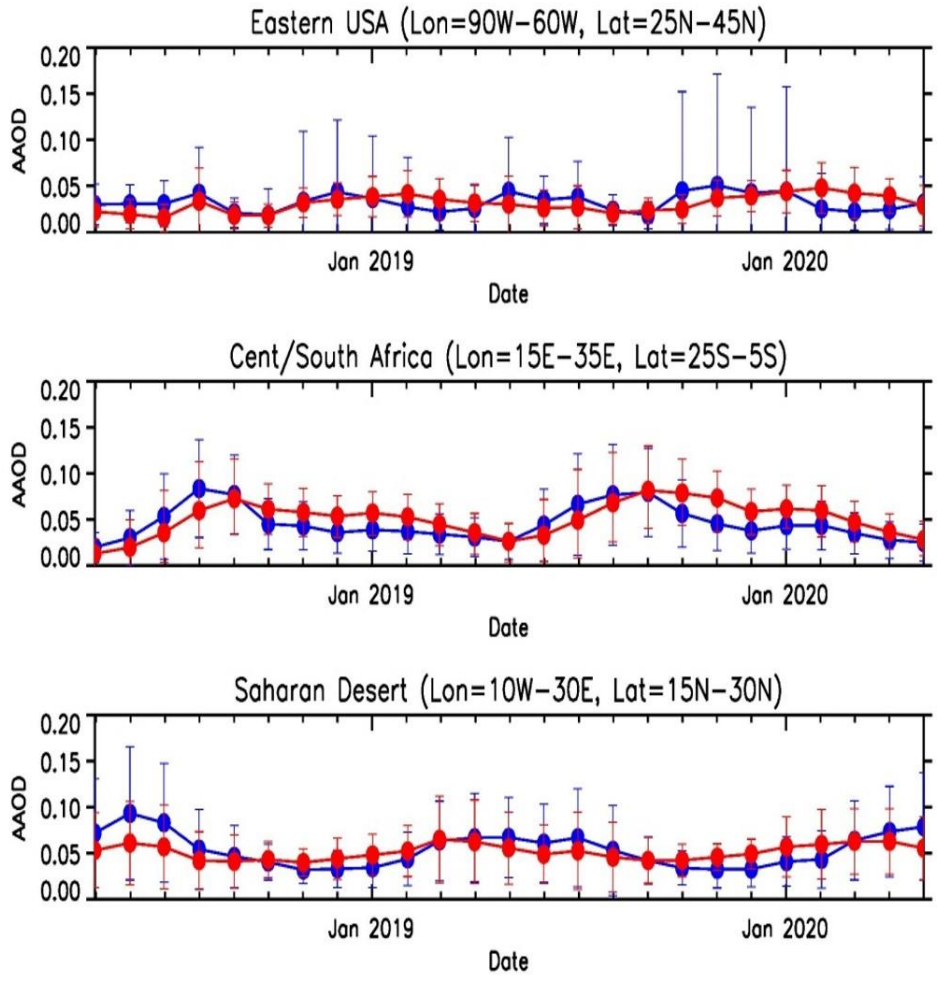

Figure 6. As in Figure 5 for AAOD.

Formatted: Font: 11 pt

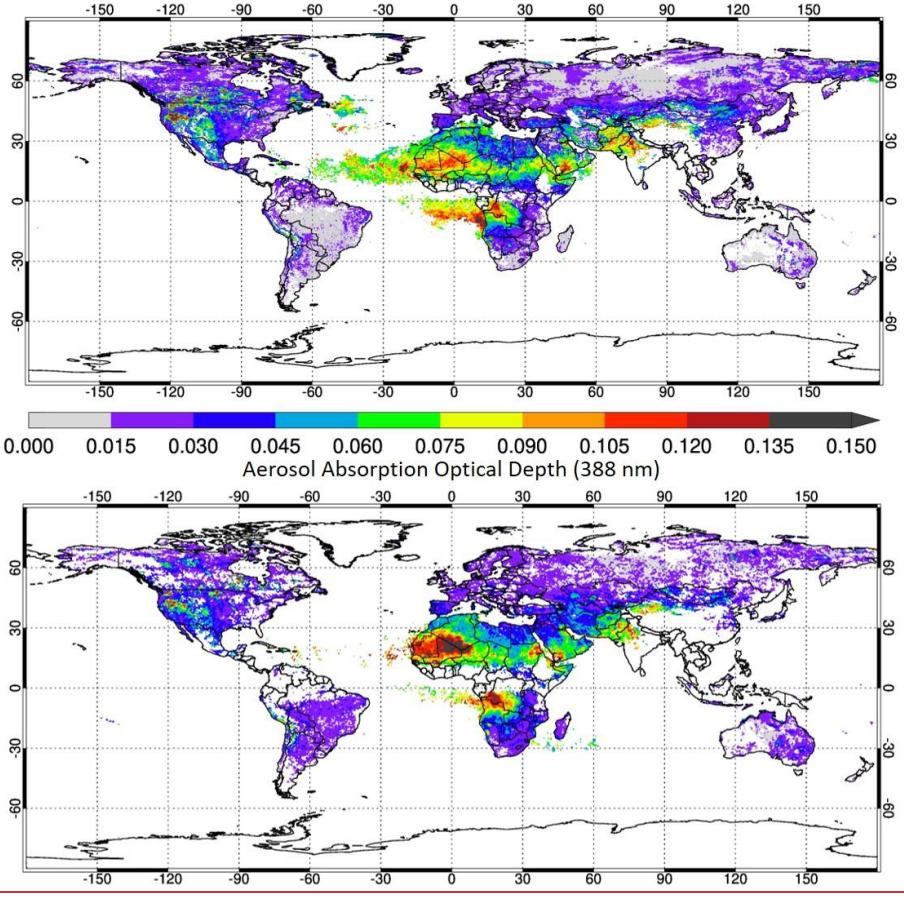

Figure 7. ~~2:~~ NH Summer Season (June-July-August 2018) global map Aerosol Absorption Optical Depth from TROPOMI ~~**Single Scattering Albedo comparison to AERONET**~~(top) and OMI (bottom) observations.

Formatted: Font: 11 pt

Formatted: Line spacing: Multiple 1.15 li

Formatted: Font: 11 pt, Not Bold

Formatted: Font: 11 pt, Not Bold

Formatted: Font: 11 pt, Not Bold

Formatted: Font: 11 pt, Not Bold

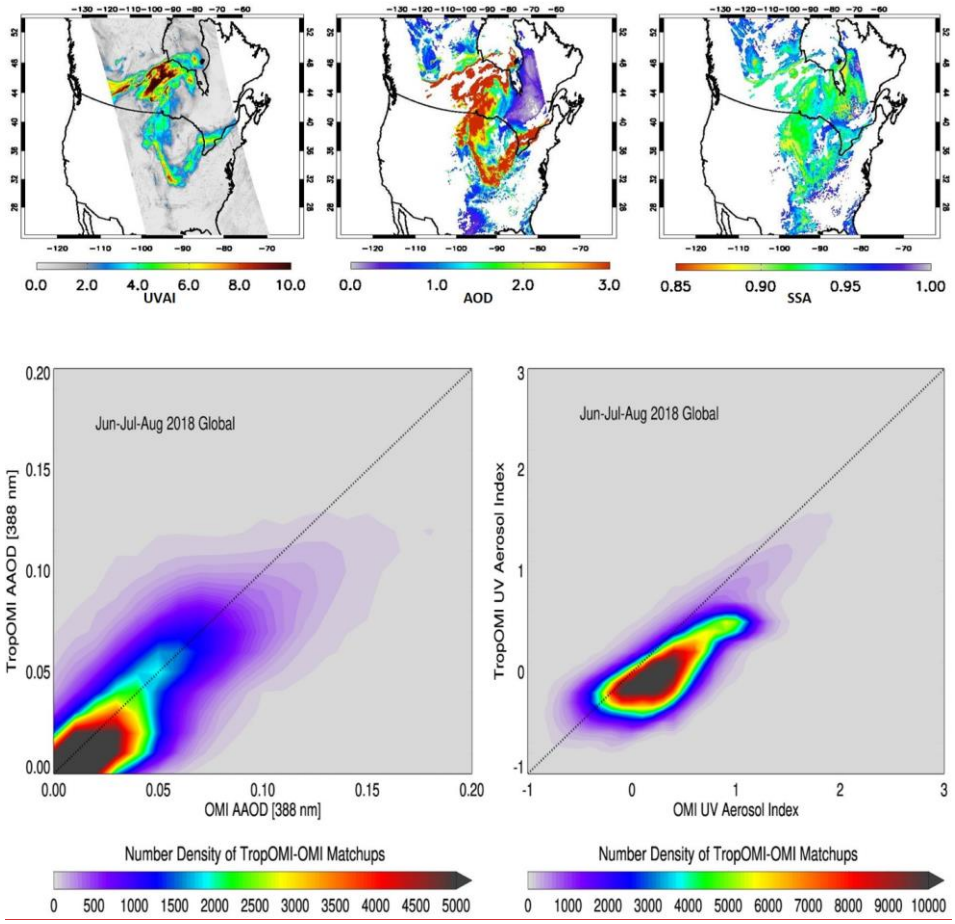

Figure ~~3.~~8. Density plots of OMI (x-axis) and TROPOMI ~~**UV Aerosol Index**~~(y-axis) gridded monthly mean (June, July, August 2018) values of AAOD (left~~**), Aerosol Optical Depth (center), and Aerosol Single Scattering Albedo**~~) and UVAI (right~~**) for carbonaceous aerosol plume during California fires**~~). Dotted line indicates one-to-one line of agreement.

Formatted: Font: 11 pt

Formatted: Font: 11 pt, Not Bold

Formatted: Font: 11 pt, Not Bold

Formatted: Font: 11 pt, Not Bold

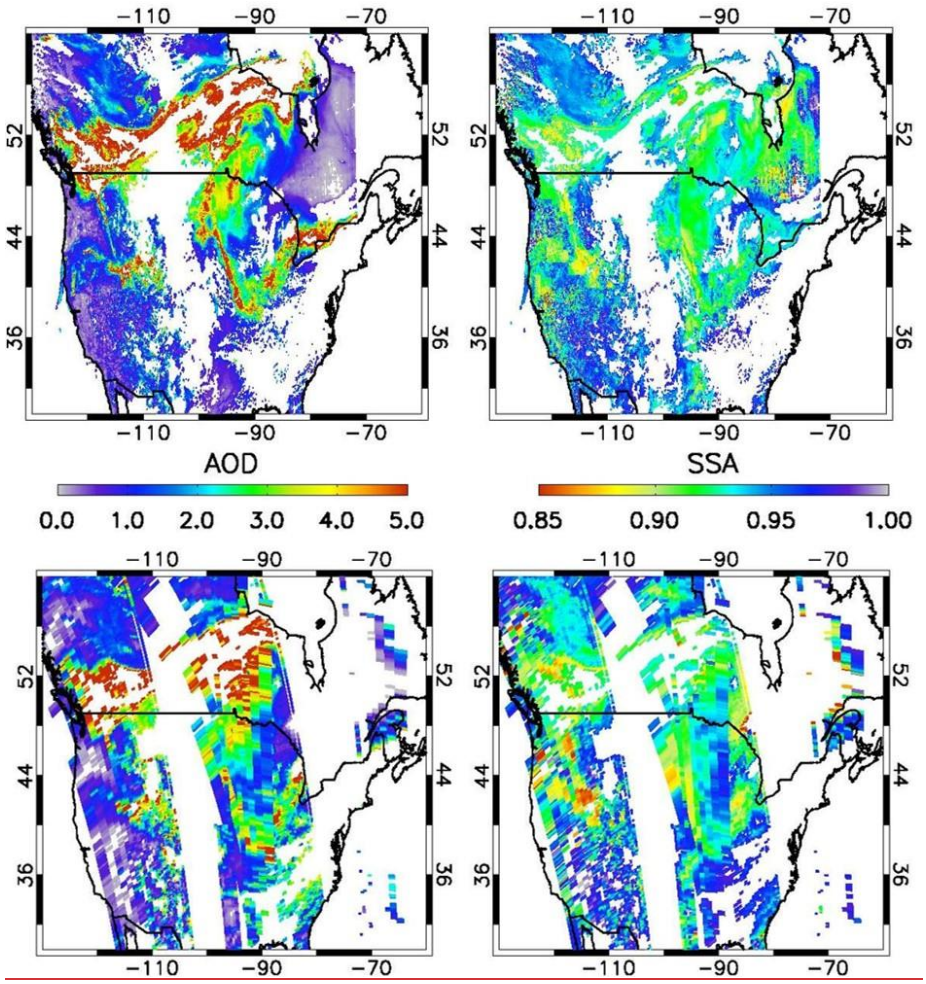

Figure 9. Spatial Distribution of AOD (left) and SSA (right) on August 18, 2018. derived from TROPOMI (top) and OMI (bottom) observations.

Formatted: Line spacing: Multiple 1.15 li

Formatted: Font: 11 pt, Not Bold

Formatted: Font: 11 pt, Not Bold

1

2

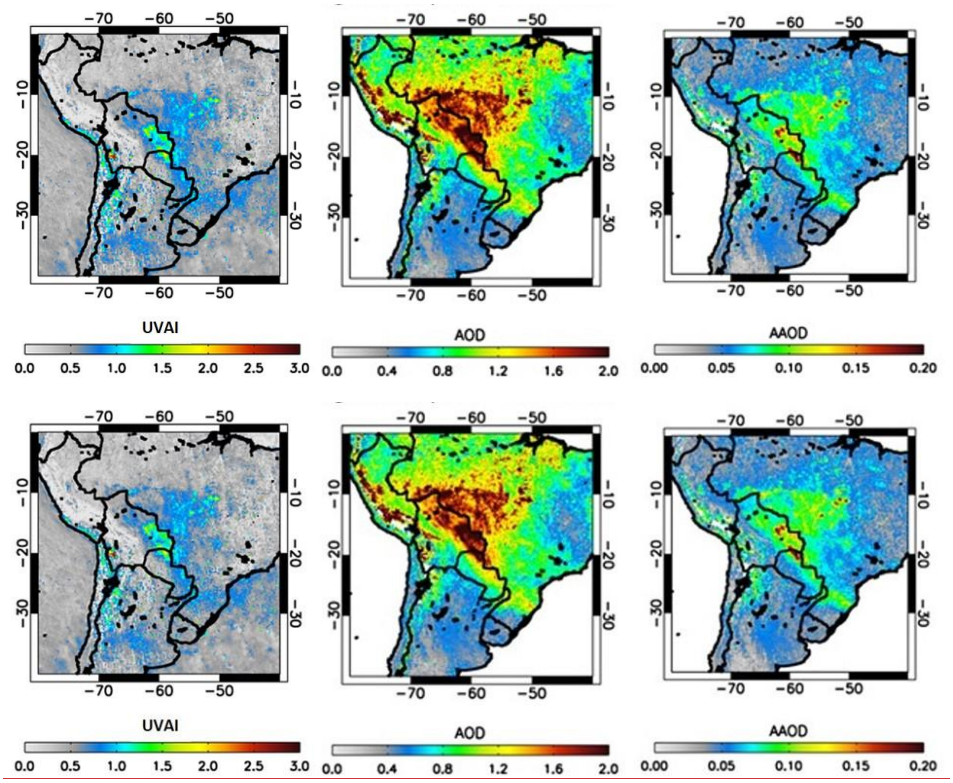

Figure 410. September 2019 monthly average values of TROPOMI ~~UV Aerosol Index~~UVAI (left), ~~Aerosol Optical Depth~~AOD (center~~),~~ and ~~Aerosol Absorption Optical Depth~~AAOD (right) ~~for carbonaceous aerosols~~ over ~~the Amazon Basin.~~South America.

Formatted: Font: 11 pt
Formatted: Font: 11 pt, Not Bold
Formatted: Line spacing: Multiple 1.15 li
Formatted: Font: 11 pt
Formatted: Font: 11 pt, Not Bold
Formatted: Font: 11 pt, Not Bold
Formatted: Font: 11 pt, Not Bold
Formatted: Font: 11 pt, Not Bold
Formatted: Font: 11 pt, Not Bold
Formatted: Font: 11 pt, Not Bold
Formatted: Font: 11 pt, Not Bold
Formatted: Font: 11 pt, Not Bold

1

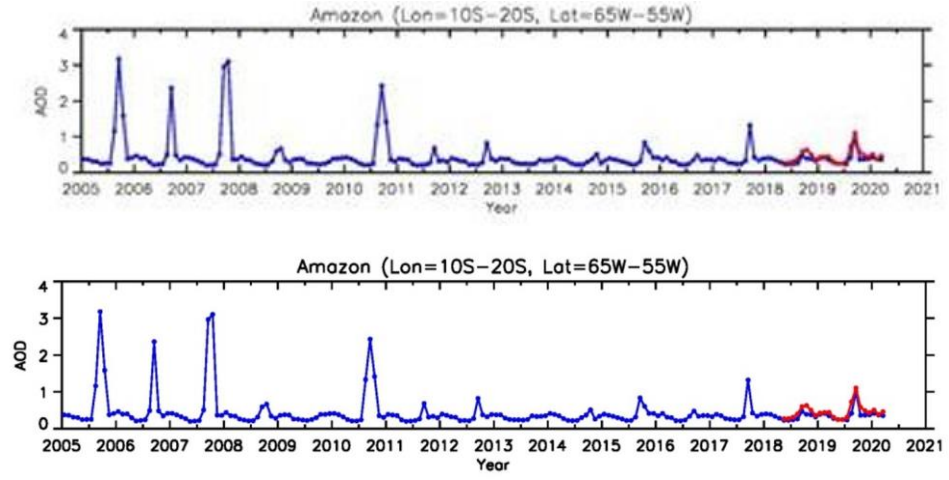

Amazon (Lon=10S-20S, Lat=65W-55W)
AOD
Year
2005 2006 2007 2008 2009 2010 2011 2012 2013 2014 2015 2016 2017 2018 2019 2020 2021
0 1 2 3 4

Figure ~~5:~~11. Time series of AOD over the amazon basin from OMI (~~**black**~~blue line) and TROPOMI (red line) observations.

Formatted: Font: Not Bold

Formatted: Font: Not Bold

Formatted: Font: Not Bold

Formatted: Line spacing: Multiple 1.15 li

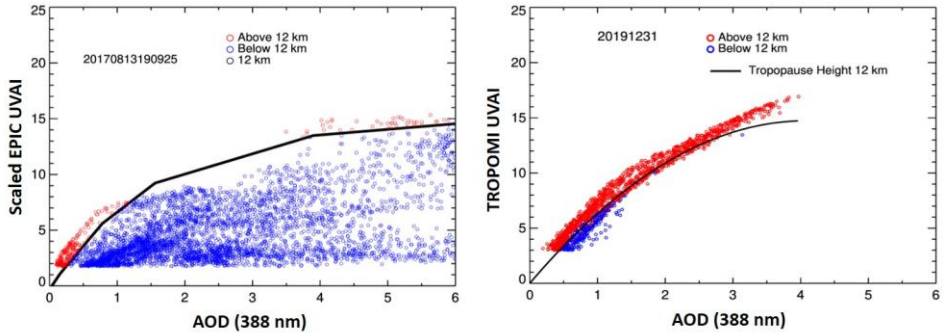

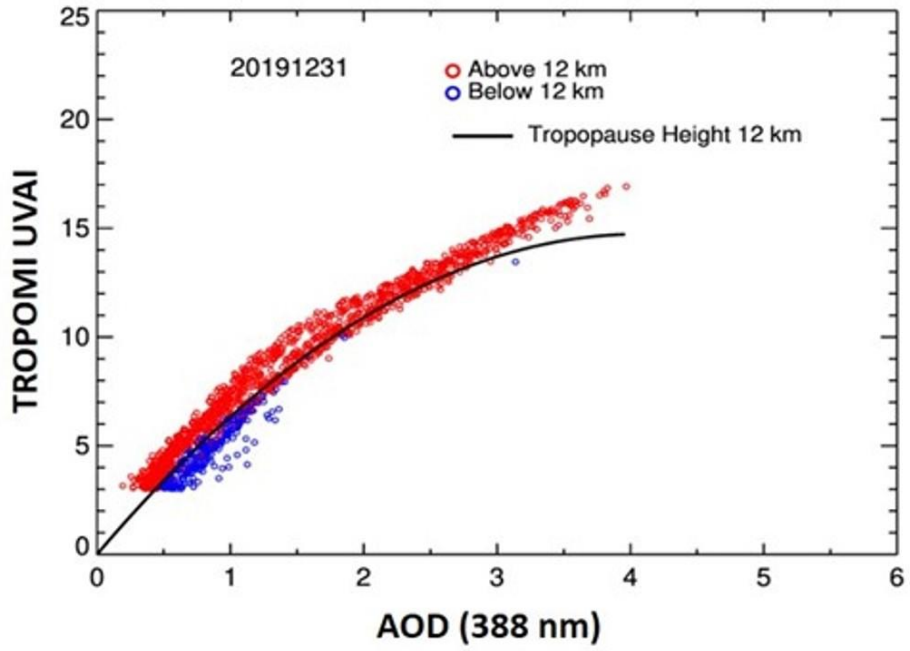

Figure ~~**6: Comparison of**~~**12.** UVAI-AOD relationship at ALH 12 km for the ~~**2017 Canadian fires (left) and**~~ 2019-2020 Australian fires (~~**right).**~~black line) on December 31, 2019. Red symbols represent aerosol retrievals at 12 km and higher. Blue symbols indicate retrievals at heights lower than 12 km.

Formatted: Font: Not Bold

Formatted: Font: Not Bold

Formatted: Font: Not Bold

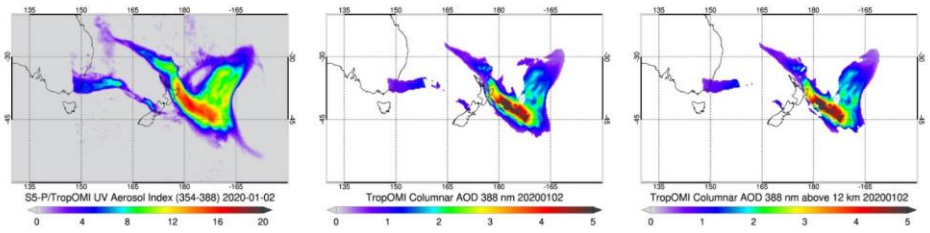

~~Figure 7.~~

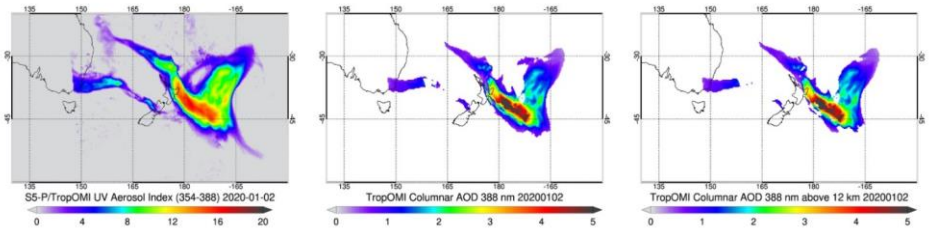

Figure 13. TROPOMI UVAI (left), total column AOD (center) and above 12 km AOD (right) fields of Australian smoke plume on January 2, 2020.

Formatted: Font: 11 pt

Formatted: Font: 11 pt, Not Bold

Formatted: Font: Not Bold

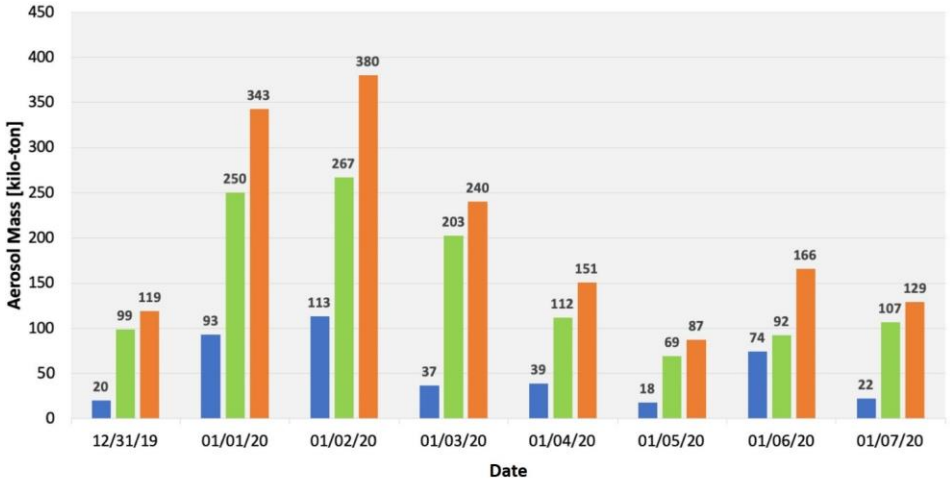

Figure ~~8. Injected~~14. Calculated Daily aerosol mass (kilotons) in the stratosphere from TROPOMI observations~~.~~, from December 31, 2019 to January 7, 2020. Results are reported for aerosols in cloud-free conditions (blue bars), aerosol above cloudy scenes (green bars), and their sum (orange bars).

Formatted: Font: 10 pt, Not Bold

Formatted: Font: Not Bold

Formatted: Font: Not Bold

Appendix A

Extinction to mass conversion

The total aerosol mass injected in the stratosphere, M, can be estimated by converting stratospheric AOD ($\tau_{str,}$ see below) into an equivalent aerosol mass per unit area, using the equation (Krotkov et al., 1999)

$$M = \Sigma \frac{4}{3} \rho r_{eff} A \tau_{str} f\left(r_{eff}\right) \qquad \text{(A-1)}$$

that yields the summation of the aerosol mass over the total area covered by the aerosol plume. In Equation A-1, ρ is the aerosol particle mass density in g-cm^{-3}, r_{eff} is the effective radius (μm) associated with the particle size distribution (van de Hulst, 1957), A is the effective geographical area in km^2, associated with retrieved stratospheric AOD, and $f(r_{eff})$ is a dimensionless extinction-to-mass conversion factor, averaging over particle size distribution, defined as

$$f = \int_0^\infty r^2 n(r) \partial r \Big/ \int_0^\infty r^2 Q_{ext}(r) n(r) \partial r \qquad \text{(A-2)}$$

where $n(r)dr$ is the assumed number particle size distribution and $Q_{ext}(r)$ is the extinction efficiency factor calculated using Mie theory. Calculations were carried out for particle mass density values of 0.79 and 1.53 g-cm^{-3} which cover the range of values reported in the literature (Reid et al., 2005).